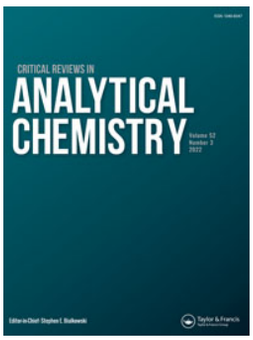

Taylor & Francis
Taylor & Francis Group

Critical Reviews in Analytical Chemistry

ISSN: (Print) (Online) Journal homepage: https://www.tandfonline.com/loi/batc20

Surface-Enhanced Raman Spectroscopy and Electrochemistry: The Ultimate Chemical Sensing and Manipulation Combination

Anna Lipovka, Maxim Fatkullin, Andrey Averkiev, Marina Pavlova, Anurag Adiraju, Saddam Weheabby, Ammar Al-Hamry, Olfa Kanoun, Igor Pašti, Tamara Lazarevic-Pasti, Raul D. Rodriguez & Evgeniya Sheremet

To cite this article: Anna Lipovka, Maxim Fatkullin, Andrey Averkiev, Marina Pavlova, Anurag Adiraju, Saddam Weheabby, Ammar Al-Hamry, Olfa Kanoun, Igor Pašti, Tamara Lazarevic-Pasti, Raul D. Rodriguez & Evgeniya Sheremet (2022): Surface-Enhanced Raman Spectroscopy and Electrochemistry: The Ultimate Chemical Sensing and Manipulation Combination, Critical Reviews in Analytical Chemistry, DOI: 10.1080/10408347.2022.2063683

To link to this article: https://doi.org/10.1080/10408347.2022.2063683

Published online: 18 Apr 2022.

CRITICAL REVIEWS IN ANALYTICAL CHEMISTRY
https://doi.org/10.1080/10408347.2022.2063683

Taylor & Francis
Taylor & Francis Group

REVIEW ARTICLE

Surface-Enhanced Raman Spectroscopy and Electrochemistry: The Ultimate Chemical Sensing and Manipulation Combination

Anna Lipovka[a], Maxim Fatkullin[a], Andrey Averkiev[a], Marina Pavlova[a], Anurag Adiraju[b], Saddam Weheabby[b], Ammar Al-Hamry[b], Olfa Kanoun[b], Igor Pašti[c], Tamara Lazarevic-Pasti[d], Raul D. Rodriguez[a], and Evgeniya Sheremet[a]

[a]Tomsk Polytechnic University, Tomsk, Russia; [b]Technische Universität Chemnitz, Chemnitz, Germany; [c]Faculty of Physical Chemistry, University of Belgrade, Belgrade, Serbia; [d]Department of Physical Chemistry, "VINČA" Institute of Nuclear Sciences - National Institute of the Republic of Serbia, University of Belgrade, Vinca, Serbia

ABSTRACT

One of the lessons we learned from the COVID-19 pandemic is that the need for ultrasensitive detection systems is now more critical than ever. While sensors' sensitivity, portability, selectivity, and low cost are crucial, new ways to couple synergistic methods enable the highest performance levels. This review article critically discusses the synergetic combinations of optical and electrochemical methods. We also discuss three key application fields—energy, biomedicine, and environment. Finally, we selected the most promising approaches and examples, the open challenges in sensing, and ways to overcome them. We expect this work to set a clear reference for developing and understanding strategies, pros and cons of different combinations of electrochemical and optical sensors integrated into a single device.

KEYWORDS

Surface-enhanced Raman spectroscopy; electrochemistry; dual-sensing; sensors; analytical methods

1. Introduction

Nowadays, a breakthrough in sensing technologies is the highly sensitive and selective multimodal chemical detection with no labeling or functionalization. Moreover, rapid and accurate analysis is critical for forensic, security, and health and natural emergencies. Here, we demonstrate that electrochemical methods (ECM) coupled with surface-enhanced Raman spectroscopy (SERS) is a promising dual-sensing combination to meet these challenges since both groups of methods can be portable, accurate, and fast. Furthermore, the simultaneous use of these approaches allows the analysis of complex multi-component probes with the data serving as each other's control. Moreover, each of them can induce specific chemical modifications that can, in turn, be monitored by the other method providing unique insights into photocatalytic and electrochemical reaction mechanisms, as well as applying a potential bias to further enhance SERS signals.

ECM have been combined with several optical methods such as luminescence,[1] fluorescence microscopy,[2] surface plasmon resonance,[3] and surface-, tip-, and shell-isolated nanoparticle-enhanced Raman spectroscopy (SERS, TERS, and SHINERS, respectively).[4–6] These combinations reveal crucial information about electrochemical phenomena such as reaction mechanism and intermediates,[7] surface and electrocatalyst homogeneity, and heterogeneity.[8] Apart from understanding the nature of the processes, optical methods[9] have been used to enhance electrochemical sensors' performance and electron transfer,[10,11] while the electrochemical sensor itself consists of a receptor, analyte, and electrode, working as a transducer to convert the reaction between an electrode and analyte into an electrical signal.

Despite multiple options, some methods are preferable to use in conjunction because of their exclusive advantages. For instance, Raman spectroscopy provides molecular fingerprints of the sample components but accurate quantitative estimation is challenging. On the other hand, ECM gives limited chemical specificity but provides quantitative measurements by following the changes in the current response. However, this already beneficial coupling still could be improved. In the 70 s, Fleishmann and coworkers discovered inexplicably high Raman signal intensity of pyridine on Ag/AgCl electrodes during an electrochemical experiment.[12] This effect was later named surface-enhanced Raman spectroscopy (SERS) and was explained by plasmon excitation on the rough silver surface. The SERS sensor is composed of a SERS-active substrate (generally with the incorporation of noble metals), which amplifies the Raman signal from the adsorbed analyte molecules with the detection limits down to the level of individual molecules. It launched a new era of research involving nanoparticles (NPs) to enhance Raman signals that conveniently increase the sensitivity of electrochemical detection. Currently, electrochemistry coupled with SERS (EC-SERS) is typically used for detecting and explaining chemical phenomena or as a

CONTACT Raul D. Rodriguez raul@tpu.ru Tomsk Polytechnic University 30 Lenin Ave, 634050 Tomsk, Russia.

way to improve device sensitivity. Moreover, combining ECM with SERS is an efficient way to monitor electrochemical reactions at ultra-low concentrations. For example, an electrical potential can promote adsorption of target analytes to the surface of noble metals, increasing the number of analytes in electromagnetic hotspots and thereby increasing the SERS limit of detection (LOD).

There are several reviews focused on combinations of electrochemical and optical methods,[9,13–18] including the recent one focusing on EC-SERS in analytical applications.[19] However, these works have either focused on (1) improving the sensitivity of one method by employing another one or (2) understanding the sensing mechanisms and surface reactions in the sensing process by complementary approaches. Moreover, there are no systematic studies on the capabilities and limits of combining these two approaches. Previous reviews highlight the dual transduction by optical and electrochemical techniques rather than methods' complementarity and interaction.

This review focuses on the dual transduction by electroanalytical techniques and SERS. We emphasize the interplay between the two techniques and show their implementation in biomedical, environmental, and energy applications. Additionally, we discuss the effect of ECM on SERS performance and vice-versa.

2. Methods description

Conceptually, combining electrochemical methods and SERS is highly beneficial, but designing an experiment suitable for both methods based on different working principles is challenging. Furthermore, the joint use of the two approaches requires a deep fundamental understanding of the physicochemical processes and specific experimental implementation discussed in this section.

2.1. Basics of electrochemical methods

Electrochemical methods are nowadays widely used in fundamental research and commercial applications. Many research papers focus on electrochemical sensors and their applications, emphasizing their portability, ease of use, high sensitivity, and low cost.[20] Besides addressing fundamental aspects in academic research, commercial electrochemical sensors are also available. These sensors are applied to detect arsenic (FREDsense), nitrate, oxygen, and phosphate (Zimmer and Peacock), ammonia, fluorine, and chlorine in water (Scan Messtechnik GmbH), as well as to monitor glucose, gasses, and metabolites (Abbott) in blood, to name a few.

Electrochemistry is the interplay between electricity and chemistry, occurring on an electronic|ionic conductor interface (electrode). The quantification of currents provides indirect information about the concentrations of electroactive species. Namely, in electrochemistry, the measured current is directly proportional to the rate of an (electro)chemical reaction, which, on the other hand, is proportional to the concentration of reactants. In turn, the voltage related to the change of the Gibbs free energy of an electrochemical reaction provides information about thermodynamics and, thus, the chemical identity of reactants, but also the concentration, as in potentiometric measurements (such as the measurement of pH).

The electronic/ionic conductor interface (the electrode in its true meaning) is a complex unit. The extreme electric fields of 10^8 V m^{-1}, which are almost impossible to form in a laboratory, are taking place at the electrode. It happens because of the formation of an electric double layer (EDL) at the interface between the electrode surface and the analyte to balance the electrode's surface charge.[21] EDL thickness and structure depend on the electrolyte composition and concentration and could be described using the Stern, Helmholtz, and Gouy-Chapman models.[22,23] EDL is composed of an inner Helmholtz layer or Stern layer, outer Helmholtz layer, and diffuse layer, while the Stern layer is composed of solvent molecules (water) and specifically adsorbed ions. Water molecules, being dipoles by nature, orient themself in accordance with the charge on the electrode surface. The outer Helmholtz layer consists of solvated ions coming from the solution operating at a distance limited by the size of the solvated shell. After the outer Helmholtz layer, there is the diffuse layer wherein the free ions can easily move inside the solution. Any electrochemically active species has to get through the EDL and approach the electronic conductor surface to undergo the electrochemical transformation. This process, in most cases, involves a direct interaction of electroactive species with the surface of an electronic conductor.

In a potential controlled technique, an electric potential applied to the electrode drives the chemical reactions, and the resulting current is measured. Colloquially, the electric potential is analogous to the wavelength in optical setups.[24,25] One of the conditions to apply any electrochemical techniques is that the analyte must be electro-active so that the redox reactions can occur. The number of electrons transferred during the redox reactions at a specific applied potential increases the current, proportional to the concentration of electroactive species in the electrolyte solution. Two key processes determining the rate of redox reactions are (1) mass transport from the bulk electrolyte to an electrode and (2) electron transfer at an electrode to the electroactive species or *vice versa* (Figure 1). (1) The mass transport of electroactive species and ions from bulk to the electrode surface can happen by diffusion, convection, and migration. The dominance of one phenomenon over the other entirely depends on the experimental conditions and the chemical nature of an electrolytic solution.[26] (2) The electron transfer takes place at the electrode/electrolyte interface when the overpotential reaches the activation energy. Overpotential value is defined by the electrode material, its surface properties, and the analyte composition.

A typical setup for electrochemical kinetics and analytical measurements consists of three electrodes: working electrode (WE), counter electrode (CE), and reference electrode (RE), as shown schematically in Figure 1. Such a three-electrode setup can be made either in an electrochemical cell or in a

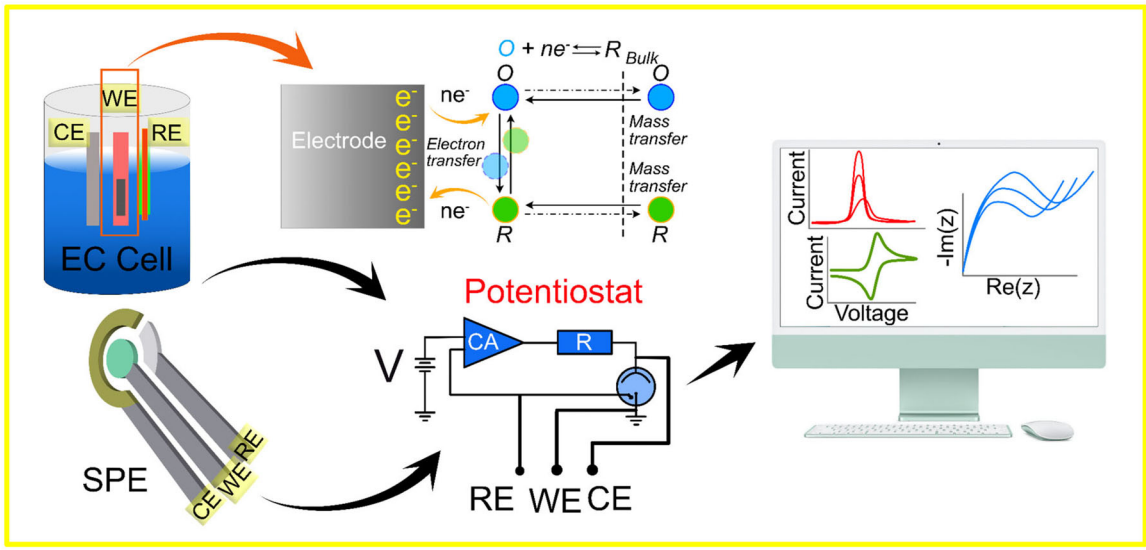

Figure 1. Schematic illustration of the experimental setup for electrochemical sensors. A three-electrode setup can be implemented in an electrochemical cell or on the surface of a screen-printed electrode. WE, CE, and RE are contacted to a potentiostat so that various EC techniques can be applied (e.g., square-wave voltammetry (SWV), electrochemical impedance spectroscopy (EIS), or cyclic voltammetry (CV)).

compact form using, for example, screen-printed electrodes (SPE). The electrodes are connected to the potentiostat, which controls the voltage or current depending on the type of measurement. Electrochemical reactions occur at the surface of WE when a varying or constant potential/current is applied, allowing the detection of the target analytes from the current/potential response. CE closes the electrical circuit with the WE, allowing the current to flow.[27] In a three-electrode setup, there is no current flow through the RE; thus, RE is at a constant potential. Hence, it is used to measure the potential of the WE during its polarization in an electrochemical experiment.[28] Electrochemical methods are classified into potentiometric,[29] coulometric,[30] voltametric,[31] and amperometric,[32] based on the type of input signal applied and/or measured quantity such as current, voltage, or charge to quantify the analyte concentration indirectly or to understand its reactivity on the surface. Most of the electrochemical measurements rely on the application of voltametric techniques, with cyclic voltammetry (CV) being the most widespread in the study of fundamental electrochemical processes and mechanisms, as well as in sensing applications. In CV, the potential is swept from a chosen point with a constant sweep rate (usually tens of mV per second), to a given vertex potential and back. Without going into the theory of CV, we note that the current response can be used to identify the nature of the rate-determining step, rate constant, concentration, the occurrence of a chemical reaction before or after the charge transfer step, etc. Besides CV, other techniques, like chronoamperometry of chronopotentiometry, where current/potential is measured upon constant potential/current applied to the WE are frequently in use. These approaches are particularly insightful for the investigation of electrochemical systems which operate under similar conditions, like a battery discharge under constant current or voltage.

The use of EC methods helps detect the target species in the analyte and quantitatively characterize the electrode surface, electrolyte, and electrode-electrolyte interactions. In this regard, there have been several studies on using EC to detect a wide range of contaminants, such as heavy metals,[33,34], as well as pesticides,[35] nitrogen species,[36] cancer biomarkers,[37,38] viruses,[39] biomolecules (such as H_2O_2, glucose and so on),[40] arsenic species,[41] and biologically active biogenic amines.[42] At present, EC helped to achieve very low limits of detection in the order of nano- to pico-moles.

Nevertheless, electrochemical sensing alone has a few inherent drawbacks.

1. The sensitivity and selectivity of the sensor are limited by the choice of electrode material or material used to modify its surface, which in turn depends on the target molecule. In other words, the expected analyte composition must be known in advance. In addition, the presence of interfering compounds in the solution further hampers the sensor performance. WE for analytical applications can be based on carbon nanomaterials,[43] metallic NPs,[44] complex 2D nanostructures,[45,46] metal oxides,[47] biomolecules,[48,49] or polymers,[50] their composites, or more complex architectures.
2. The performance and repeatability of the electrochemical sensor are highly dependent on the structure of the electrode surface.[51,52] Thus, advanced strategies in nanotechnology to modify the electrode surface must be integrated to improve the sensors' repeatability.[52]
3. Electrochemical sensors tend to age and are fouled rapidly in complex media,[53] while the rate of aging depends on the electrode material. New strategies should be developed to prolong the sensor lifetime by implementing anti-fouling nanomaterials and electrode regeneration techniques.[54,55]

The above-mentioned complications must be mitigated to develop devices with higher repeatability and longer lifetime.

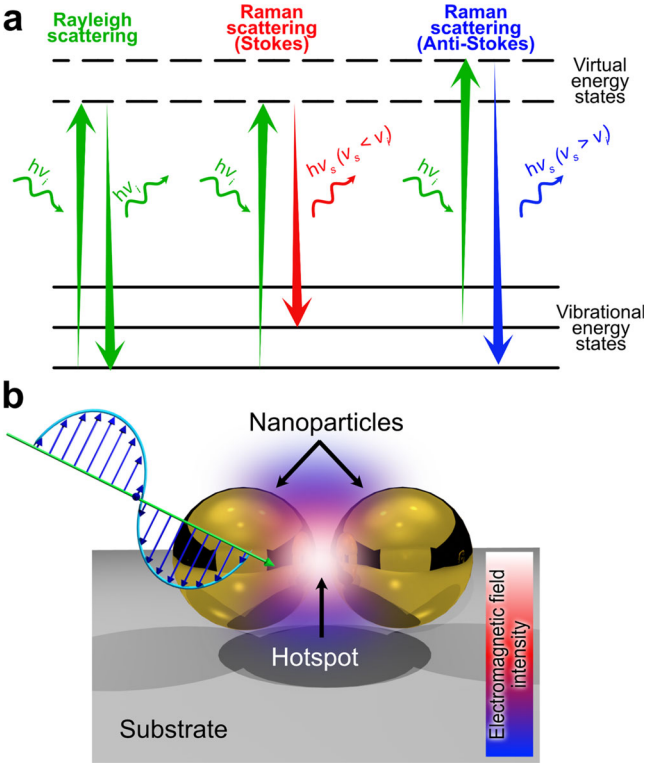

Figure 2. a) Energy diagrams for electron transitions with different types of scattering; b) Schematic principle of plasmonic enhancement of Raman signal (SERS).

Moreover, combining EC with other transduction techniques will enable us to understand the surface chemistry and changes occurring on the electrode surface during measurements. The additional information can improve the sensor performance while alleviating some inherent drawbacks related to selectivity (Figure 1).

If ECM is combined with other approaches, like Raman spectroscopy, it is necessary to properly match the time resolution and selectivity of these techniques. In other words, if there is an intention to detect products of an electrochemical reaction or their intermediates, the second technique must be capable of capturing their appearance during an electrochemical reaction. However, in contrast to chemical reaction systems, where the reaction rate is determined by the concentration of reactants, temperature, and pressure, in electrochemical systems there is an additional control parameter. This is the electrode potential, whose precise control, easily done using modern electrochemical devices, finely tunes the rate of electrochemical reaction. For this reason, EC methods seem perfect for combining with other analytical techniques.

2.2. Basics of Raman spectroscopy

Raman spectroscopy is one of the most widespread, specific, nondestructive, rapid, and informative physicochemical methods for material analysis. The underlying process of this technique, the Raman scattering effect, was discovered by C. V. Raman in 1928. Raman measurement provides a vibrational spectrum of the analyte, which can be considered as its "fingerprint" and allows its identification.[56] Being a widely-used characterization procedure, Raman is readily applicable to different classes of materials, including polymers, superconductors, semiconductors, carbonaceous, environmental materials, and others.[57] With the help of Raman spectroscopy, it became possible to analyze complex molecules and molecular systems like pharmaceutical[57] and biomedical ones.[58] One of the essential biological applications of Raman is distinguishing cancerous cells from normal tissue.[59]

There are three distinct light scattering processes. Statistically, most photons would undergo elastic or Rayleigh scattering, i.e., they will be scattered without energy change. The two types of Raman scattering—with an energy loss and energy gain—provide information about the material structure. Stokes scattering is attributed to the fact that the energy of the scattered photon $h\nu_S$ is lower than that of the incident one $h\nu_I$, while anti-Stokes scattering $h\nu_S$ is larger than $h\nu_I$. The energy change is defined by the sample's unique structure of vibronic states that provide a specific and informative spectral "fingerprint" (Figure 2a).

However, the Raman process has a very low scattering probability that results in low signal intensity. That affects the spectra quality and LOD that could be obtained straightforwardly.

The most efficient way to overcome this is through surface-enhanced Raman spectroscopy that uses plasmonic NPs to amplify Raman signal intensity significantly. The large signal increase was initially attributed to the enlarged surface area of the electrochemically roughened silver electrode. Later on, it was postulated that the Raman signal enhancement has an electromagnetic origin.[60] Nowadays, it is generally accepted that two mechanisms enhance the Raman signal in SERS. They are the electromagnetic (EM) mechanism and the chemical (C) mechanism, with a slight impact on the enhancement from C and mostly from EM. The EM mechanism originates from the coherent oscillation of conduction electrons in noble metal nanostructures that induce the spatial confinement and amplification of the incident electric field. The C mechanism is related to the change in the Raman scattering efficiency due to molecule/metal interaction (Figure 2b). In addition to signal amplification, the relative molecular orientation with respect to the hotspot and electric field can influence the relative intensity of different Raman peaks[61] (Figure 2).

SERS measurements could be performed by mixing an addition of analyte to the colloidal NPs suspension, then depositing the mixture onto any substrate,[62,63] or the deposition of colloidal NPs directly on the analyzed sample. For example, onto a tea leaf to detect pesticides on its surface.[64] Another common way is the deposition of a target analyte to the prepared SERS active substrate.[65,66]

So far, SERS has been successfully used to detect heavy metals in water,[67,68] bacteria and biomolecules,[63,69] viral antigens,[70] drugs,[71] organic and inorganic molecules,[72] and pesticides.[73] With the help of optical forces, SERS could be used to detect molecules in liquid environments.[74,75] Among the other interesting approaches, a

Table 1. Types of EC-SERS combination.

Type of EC-SERS combination	Description	Examples in literature
Equivalent combination	Both methods are applied for detection equally and independently (sequentially or simultaneously)	[93,94,137,138,148,150,190,198]
Complementary combination	Advantages of one of the methods overcome drawbacks of another (e.g., SERS—as qualitative method, EC—as quantitative method)	[96–98,139]
EC enhancing SERS	EC is used as a method to increase the efficiency of SERS detection	[104,199–201]
SERS monitoring of EC	SERS is applied for monitoring electrochemical reactions	[105,108,109,143,202]
EC-SERS (SHINERS) monitoring of photocatalytic reactions	EC-SERS(SHINERS) for monitoring surfaces plasmon-induced SPR-induced (photocatalytic) reactions	[99,112–117]

thermophoretically driven assembly of metallic NPs for SERS detection was recently developed.[76–78] As with most sensing techniques, LOD is the key figure characterizing SERS performance in detection. For example, in the case of pesticides detection in food samples, it was possible to achieve picomoles and ppb LOD.[79]

SERS experiences challenges similar to EC measurements:

1. SERS is less prone to surface fouling because Raman spectroscopy gives fingerprint spectra, meaning that the signal from both fouling molecules and target analytes can be distinguished. Still, SERS substrates are rarely reused[80–82] due to unavoidable contamination of the surface and the challenges of refreshing it.
2. Just like EC, SERS is sensitive to the analyte volume close to the surface. Thus, it is imperative to bring the target molecules to the surface by functionalization (modification). For example, one of the common ways to verify the SERS activity is using thiols as target molecules since thiols have a very strong affinity toward noble metals used in SERS substrates.[83,84] Often, antibodies and aptamers are used to bind biological molecules, recently imprinted polymers have been introduced, metal-organic frameworks are employed for concentrating analytes close to the SERS active surface.[85,86] Also, SERS is not highly informative for heavy metal detection, even though it could be done indirectly. In this case, SERS detection is performed by following the signal changes in pre-assembled linker molecules.[72] A similar approach is used when a target molecule has a very low signal.[72]
3. SERS is extremely sensitive to the nanoscale surface structure since the highest contribution to the signal comes from the areas with the strongest electric field enhancement, the so-called "hot spots." The enhancement depends exponentially on the spacing between neighboring nanostructures.[87] In combination with the irreproducibility of the optical focusing, spacing strongly affects signal intensity,[88] making it one of the critical issues preventing SERS from becoming a commercially adopted sensing method. The ways to improve SERS reproducibility include high-precision nanofabrication technologies,[89,90] self-assembly approaches that fix the distance between NPs,[91] or the use of internal reference molecules to calibrate the analyte's signal intensity.[92]

To sum up, both ECM and SERS suffer from similar drawbacks; fortunately, some of each can be compensated by combining the two approaches as described below.

3. Combination of EC and SERS

In the simplest case, EC and SERS contribute to the detection equally (they both provide qualitative and/or quantitative analysis) synchronously but independently (*equivalent combination*, Table 1).[93] In an equivalent combination, optical and electrochemical spectra provide complementary information and serve as each other's control. The WE also serves as a SERS substrate. To implement an equivalent EC-SERS combination, our group fabricated rGO SPE on polyimide substrates with silver functionalized WE to detect 4-nitrobenzenethiol (4-NBT) as a standard thiol system usually used for estimation of photocatalytic activity and selectivity.[93] The independent use of SERS allowed us to qualitatively detect the molecule and track the photoinduced transitions of 4-NBT to 4-aminobenzenethiol (4-ABT). In addition, the use of EC confirmed the analyte nature and helped quantify the electroactive surface area of silver nanostructures. Recent works implement SPE geometry for the equivalent combination.[94,95] Castaño-Guerrero et al.[94] showed a sequential use of SERS and electrochemical impedance spectroscopy (EIS) for carcinoembryonic antigen (CEA) detection using gold nanostars for electrode modification. In this case, both methods provided helpful information, but the sensitivity of SERS was higher than that of EIS (0.25 ng mL^{-1} for EIS and 0.025 ng mL^{-1} for SERS).

Overall, the equivalent combination is one of the most widespread as it implements two types of sensing/transduction based on the same sensor materials, and such realization is easy to fabricate and implement. To improve the selectivity of both approaches, the WE can be functionalized with enzymes or antibodies. The other way is to use noble metal NPs or Au/Ag surface roughening that increases surface area and plasmonic activity. Thus, measures to boost one method also improve the performance of the other one.

The most significant limitation of SERS is that it is mostly not a quantitative detection method without additional modifications, while electrochemistry provides more options for quantitative analysis of various parameters, including the active surface area and capacitance. As a block of analytical techniques, EC could be used for concentration/activity quantification if adequately calibrated. On the

other hand, EC provides only limited information about the chemical composition of the analytes, in contrast to SERS. For instance, Sanger et al.[96] have shown the evaluation of the electrochemically active surface area (ECSA) with EC, making it possible to quantify the SERS enhancement factor for paracetamol. In biomedical settings, such a *complementary combination*, where the advantages of one method overcome the disadvantages of another (i.e., SERS provides qualitative investigation, while EC is used for quantitative analysis) (Table 1) allows one to avoid false positive and false negative results provided with two methods.[97] In the forensic analysis of cocaine, the EC response was used to quantify the amount of adulterating compounds such as paracetamol and caffeine. The results were comparable to the standard method, which is high-performance liquid chromatography. At the same time, SERS gave additional information about the presence of another pharmaceutical substance, which is used for diluting cocaine, such as levamisole.[98] Remarkably, the optimized electroactive area from EC measurements is also best for SERS performance since the EC activity of a WE depends on its composition and microstructure, which are the same parameters that affect the SERS sensitivity.[99]

Simultaneous application of electrical potential and illumination with light can lead to various modifications of the analyte and the SERS electrode. These effects are already employed to *enhance the SERS signal* by applying an external potential, *monitoring electrochemical redox reactions using SERS*, and following *photocatalytic reactions* (see Table 1).

Potential applied to the WE leads to the shift in the energy levels at the analyte-metal interface. When the Fermi level (E_F) of the electrode aligns with the highest occupied molecular orbital (HOMO)/lowest unoccupied molecular orbital (LUMO) levels of the molecule, the HOMO-E_F and E_F-LUMO transitions become resonant with the incident laser wavelength.[100] Thus, a charge transfer mechanism can be triggered between HOMO and unoccupied states above the Fermi level (or between LUMO and occupied states slightly below E_F). This process can be tuned by applying a potential to the SERS substrate until resonant conditions for the photoexcitation are reached, or electrochemically induced charge transfer can increase the Raman cross-section of the molecule, contributing to higher signal amplification.[101,102] However, when analyzing the results, one has to be aware that the Raman intensity, in that case, is no longer proportional to the molecule concentration and, thus, a quantitative analysis becomes way more challenging.

Another effect of applying the potential is the electrostatically-induced adsorption/desorption of the analyte molecules on the SERS active electrode during a potential sweep.[103] This will change the concentration profile of different species. Thus, quantification using SERS has to be carefully assessed. In this regard, Bindesri et al.[104] have shown a substantial signal enhancement obtained from *4*-Aminobenzenethiol (*4*-ABT) and levofloxacin when applying cathodic potential, with maximum signal intensity observed at −0.6 V vs. Ag/AgCl RE for both analytes. The signal remained stable with a further potential increase for levofloxacin, but it decreased for 4-ABT, especially for modes attributed to the plasmon-assisted catalytic conversion of 4-ABT to dimercaptoazobenzene (DMAB). It should be mentioned that levofloxacin is a problematic molecule for SERS detection, because of the absence of functional groups which could give a strong Raman signal. As a result, the drug signal in SERS spectra only appears with a potential increase using the SPE.[104] The concentration profile change can be counteracted by covalently linking the analyte to the electrode surface, as shown for Rhodamine 6 G (R6G) on an ITO substrate modified with silver NPs.[105] The SERS spectra are also affected by the molecule/surface adsorption geometry. Therefore, even small electrode potential changes can impact the Raman peaks intensity ratios in the SERS spectra.

The next *EC-enhanced SERS* method, which is based on the usage of EC to increase the efficiency of SERS detection, is also complicated by the possibility of changing the SERS substrate surface itself (particle size, roughness, hotspot density, surface morphology, etc.) by applying a potential (Table 1). In case of too high a positive potential, the plasmonic metallic nanostructures become oxidized, and the SERS substrate could become inactive. Such an effect can be mitigated by taking into account the potential window of the SERS active WE. On the other hand, silver electrodes could be restored and cleaned from tarnish or other contaminants by applying constant negative potential or making several potentiodynamic cycles.[106] Similarly, depending on the voltammetry scanning parameters, a silver electrode could be roughened,[107] increasing the hotspot density that contributes the most to the Raman signal amplification. Yang et al. have shown the *in situ* monitoring of the electrodeposition of copper on a glassy carbon electrode using SERS with R6G as a Raman probe.[108] The different stages of the electrodeposition process of copper, such as the nucleation stage, formation of aggregates, and shape change of the copper NPs, directly affect SERS enhancement, indirectly monitoring the process of EC deposition of the plasmonically active metal.

The other experimental issue combining EC and SERS is that the effects on electrochemical doping or modifications of the electrode material cannot be avoided since the potential change of the WE is needed to record a voltammogram.[105] In this case, *SERS monitoring of EC* combination could be applied for tracking the electrochemical activity (Table 1). For example, SERS could be used for *in situ* monitoring of the intensity changes in N-O stretching mode, indicating the electrocatalytic reduction processes of the nitrate ion.[108] In this case, the chemical changes are irreversible, and the obtained SERS spectrum represents the electrochemically reduced system rather than the original mixture. On the bright side, SERS signals or fingerprints of the molecules could give us information about the chemical reactions happening on the surface at a particular potential. In one other work,[109] time-resolved SERS was implemented to monitor the intermediates of carbon dioxide reduction reactions with millisecond resolution and surface

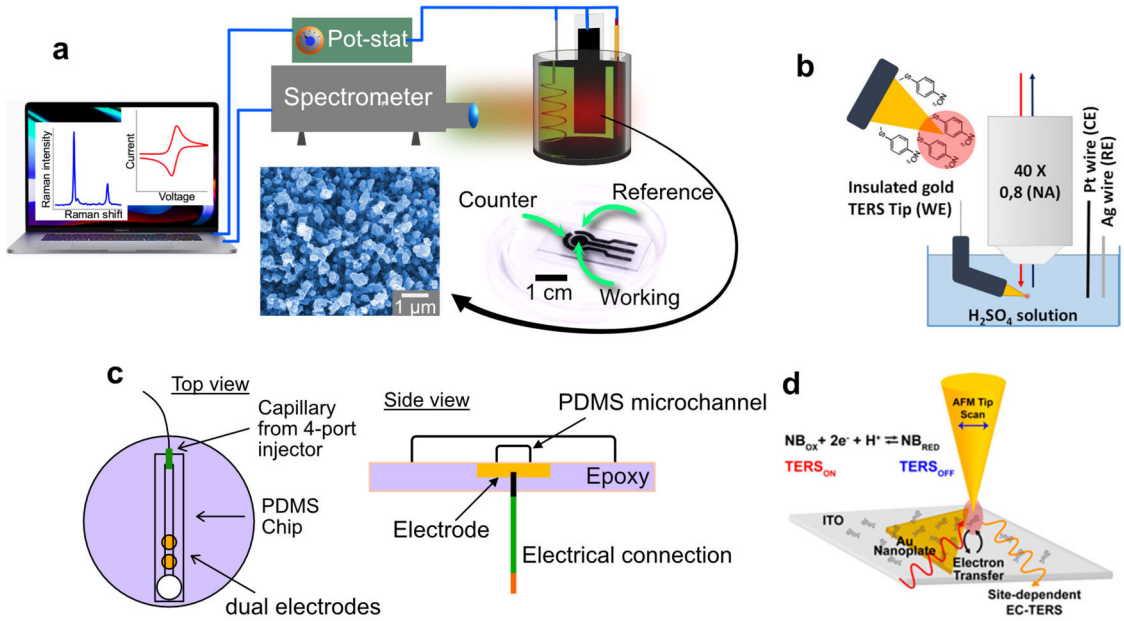

Figure 3. Experimental setups for spectroelectrochemistry. a) Direct focusing of a laser beam on the WE of SPE immersed in a vial with targeted analyte;[120,121] b) Focusing using water-immersion objective. Adapted with permission from Ref. [122] Copyright (2017) American Chemical Society, c) Focusing on a disk electrode through a microfluidic channel;[123] d) EC-TERS setup. Adapted with permission from Ref. [124] Copyright (2019) American Chemical Society.

changes of the copper substrate. In principle, EC can assist SERS detection by modifying the original molecule through a Faradaic process and making a product with a much higher Raman activity (potential-driven chemical enhancement).[110,111] It is instrumental when the original analyte has a very low Raman cross-section, making the simple detection of minute quantities impossible (Table 1).

Like the applied potential, sample illumination in the SERS experiment can induce photochemical reactions, sometimes unforeseen ones.[99,112] SERS itself could assist the interpretation of such photochemical processes whenever they are visible in the Raman spectra.[99,113] For example, Zhao et al. investigated the conversion of pyridine to bipyridine by C–C coupling triggered by surface plasmon resonance (SPR) -assisted electrocatalytic transformation. The duration of laser irradiation and electrode potential was controlled during the SERS spectra acquisition to confirm the improved efficiency of dimerization properties due to SPR excitation and applied potential.[113] If that happens, then the EC data acquired simultaneously to SERS would not represent the original analyte under investigation and could be misinterpreted. Information about the molecule's electronic properties, attention to electronic or molecular transitions that could be excited by the Raman laser, and the use of proper controls help mitigate this effect.

For such a situation, *EC-SERS (SHINERS) monitoring of photocatalytic reactions* could be used to study SPR-induced and photocatalytic reactions to suppress undesired effects (Table 1). Inadvertent charge transfer and photocatalytic reactions could be minimized, for example, using SHINERS, which are plasmonic NPs coated by a thin silica layer so that the SERS active metal NPs at the core do not influence electrochemical reactions.[114–117] This approach makes characterizations of plasmon-induced photocatalytic or photoelectrocatalytic reactions more reliable. This strategy could also help minimize the effects of protein denaturation or biomolecule decomposition when using metals as SERS substrates or electrochemically active materials. However, SHINERS can also act as a physical barrier between the analyte in the bulk electrolyte and a WE, affecting mass transport and electrochemical reaction kinetics.

Finally, EC combined with SERS could provide multiple insights into reaction kinetics and intermediates, while changing experimental conditions could enhance the signal in both approaches.

4. Experimental implementation

The combination of EC and optical techniques can be categorized into *ex situ* and *in situ* methods. *Ex situ* approaches involve spectroscopic measurements outside the electrochemical system. On the other hand, *in situ* methods require the integration and measurement of electrochemical and optical techniques simultaneously and directly in the electrochemical system.[118] *In situ* methods, also referred to as spectroelectrochemistry, have been used to monitor electrode reactions, surface processes, and the formation of intermediates in electrochemical reactions.[96,119]

Most of the EC-SERS combinations mentioned in the previous section, except the equivalent combination performed sequentially, require simultaneous implementation of both methods. It means that SERS should be performed in a liquid medium, which could be challenging as it requires using a laser beam on a WE surface through the electrolytic solution. There are currently several experimental setups to perform such measurements, avoiding crucial sacrifice of signal enhancement and sensitivity (Figure 3).

The first way is to focus the laser beam directly through the liquid in an EC cell.[125] The second approach is fabricating a custom-made photoelectrochemical cell with a

Table 2. EC-SERS sensors in Biomedical Applications.

Analyte	Substrate (WE)	Functionalization	LOD	Analytical range	RSTD/reproducibility	Selectivity	Time of analysis	Reference	Comments
CEA and AFP	Gold microarray electrode	Ab2-AuNPs-CDNA	EC: CEA 0.01 ng mL^{-1} AFP 8.0 pg mL^{-1} SERS: CEA 0.6 pg mL^{-1} AFP 0.3 pg mL^{-1}	EC: CEA 0.04–10 ng mL^{-1} AFP 0.03–6.0 ng mL^{-1} SERS: CEA 5–200 pg mL^{-1} AFP 2–100 pg mL^{-1}	RSTD within 6 sensors less than 10%	EC: peaks from DA, AA and UA are separate	–	[137]	Sensitivity: EC: CEA 1.10 uA $ng^{-1} mL^{-1}$ AFP 2.38 uA $ng^{-1} mL^{-1}$
miRNA	Popcorn-like gold nanofilms	SH-DNA	EC: 2.2 fM SERS: 0.12 fM	EC: 5 fm–100 pm SERS: 0.5 fm–0.5 pm	RSTD of intensity in map from one sample 3.6%	Signal of the target miRNA has the most significant enhancement over six types of miRNA		[138]	
DOX	Gold-disk electrode	CYS/rGO/AuNP/pDNA	EC: DOX 0.008 mg/mL, for S/N ratio 3:1 ($\sigma = 0.323$ μA, n = 11)	EC: DOX 0.003 to 5 mg/mL	EC: for 1 mg/mL DOX 3.42% ($\Delta ip = 6.43 \pm 0.22$ μA, n = 5)	The signal is highly specific depending on the chosen vibrational mode. Raman tags were not used. SERS sensing is based on the recognition of Raman vibrations of molecules.	–	[139]	SERS signal averaging over a 5 μm line length on the sample was used, averaging 10 spectra
Uric acid	Au/Ag on the carbon SPE	–	not studied	0.1–1.0 mM	Relative errors $\leq$17%	A linear relationship between the SERS signal intensity at 634 cm^{-1} and the uric acid concentration	30 s	[142]	EC-SERS spectra collected at −0.9 V vs Ag/AgCl
CEA	Au-SPE	Cysteamine layer for EIS; AuNS were modified with 4-aminothiophenol for SERS	–	0.25 to 250 ng/mL	Linear correlation coefficient of 0.991	Selectivity against creatinine and glucose	For SERS: integration time of 2 s and 5 accumulations	[94,138]	
Levofloxacin	Cotton blend fabric modified with AgNPs and conductive inks	KCl		0.45 to 1.8 mM		EC-SERS signal obtained at −0.6 V vs Ag/AgCl for levofloxacin in 0.1 M NaF		[98,104]	
Cystatin C	Au coated silicon nanopillar substrate	thiol-ended antibody fragments	1 pM and 62.5 nM by SERS and DPV respectively in	9.66×10^{-8} M (n = 6) concentration in 20 μL of	RSD = 3.8% for SERS (n = 15).		–	[143]	

			human blood plasma	human blood plasma					
Tuberculosis (TB) DNA	AgNPs on commercial SPE	5′ thiol	280 mg mL^{-1}				EC: increments of 0.1 V for a time interval of 60 seconds	[144]	
6-TUA	AgNPs functionalized SPE	Pretreatment strategy with chloride ion	μM levels, still detectable at 1.0 μM	μM range	–	Selective toward 6-TUA. Selectivity was confirmed by testing in NaF and synthetic urine, spectra represented by 6-TUA and show no difference in both cases	30–60 seconds depending on power	[146]	Portable EC-SERS system
Caffeine and paraxanthine	Ag		15 μM for paraxanthine	2 mg/kg and 3.5 mg/kg were ingested by volunteers		Only two spectral bands located at 692 cm^{-1} and 2930 cm^{-1} out of the all the bands could be used as the potential spectral markers for the paraxanthine or caffeine		[147]	
Theophylline	BOB-NR	Au@SPCE	EC: DPV −0.721 nM AM 0.353 nM SERS: 0.01 nM	EC: DPV 0.001–2.011 μM AM 0.002–1.480 μM	SERS signals from 9 points at a single substrate give nearly similar intensity.			[148]	Sensitivity in EC is 5.7697 $\mu A \mu M^{-1} cm^{-2}$
Gentamicin	Au film over nanosphere	–	100 ng/mL (300 nM)	SERS 0.5–50 mg/mL (1.12–112 mM) EC 0.5–50 mg/mL (1.12–112 mM)			5 s	[149]	
8-hydroxy-2′-deoxyguanosine (8-OHdG) and 8-oxo-guanine (8-OXOG)	Flexible Au electrode	PBS	For G and 8-OHdG are 5 nM and 10 nM, respectively				10 s	[151]	

CEA, carcinoembryonic antigen; AFP, *alpha*-fetoprotein; DA, dopamine; AA, ascorbic acid; UA, uric acid; miRNA, MicroRNA; BNP, B-type natriuretic peptide; 6-TUA, 6-thiouric acid; DPV, differential pulse voltammetry; AM, amperometric detection; BOB-NR, BiOBr Nano-rose architectures; SPCE, screen-printed carbon electrode

transparent window for SERS measurements. For example, a vial could serve as a photoelectrochemical cell (Figure 3a).[120,126,127] However, those methods imply two additional interfaces that could decrease the sensitivity. The third way is to use water-immersion objectives (Figure 3b).[122]

A more elegant solution is to make a microfluidic channel between the Polydimethylsiloxane-based electrodes.[123] In this case, electrodes have a disk shape, and the analyte solution is pumped through a microfluidic channel, as shown in Figure 3c. This approach is widely used to perform EC-SERS.[128,129]

Electrochemical tip-enhanced Raman spectroscopy (EC-TERS) allows performing EC and Raman spectroscopy measurements with nanometer resolution. EC-TERS uses a plasmonically active electrically insulated tip to perform simultaneous detection by both approaches. The physical principle of tip-enhanced Raman spectroscopy (TERS) is similar to that of SERS since both of these techniques are based on plasmon signal amplification. In the case of TERS, the plasmon excitation occurs at the apex of the gold or silver atomic force microscopy (AFM) or scanning tunneling microscopy tip so that the resolution is limited by the tip size and no longer by the diffraction limit. In turn, scanning electrochemical microscopy (SECM) is an AFM implementation of electrochemical measurements that reaches a tip-limited resolution of electrochemical properties.[130,131] It can probe electron, ion, and molecule transfers and other reactions at solid-liquid, liquid-liquid, and liquid-air interfaces. The tip serves as a CE, and the current is measured to characterize the electrochemical activity at the working electrode. The tip itself must be electrically insulated everywhere except the very apex to eliminate parasitic currents. SECM has been successfully used to map surface redox potential distribution, investigate electrochemical reactivity of interfaces, etc.[130,131]

EC-TERS was successfully implemented for local investigation and mapping of redox reactions/activity [124,132] with a high lateral resolution up to 8 nm,[133] monitoring of plasmon-driven reactions,[134] potential-induced molecular reorientation,[135] probing of molecular absorption.[136] However, due to the complexity of experimental implementation, there are very few experimental setups for dual EC-SERS(TERS) detection. Different experimental conditions allow for diversifying the approaches and maximizing the information obtained from the experiments. The critical part is where these methods are used and which applications they could serve.

5. Applications

The availability of the EC-SERS setups limits the wide use of this synergetic combination for practical applications. However, the benefits are worth the result. In addition to precious data, these methods afford high flexibility: the user is barely limited in the choice of experimental configuration, WE materials, and the application area. In the following section, we sort the current implementations of EC-SERS into three categories: biomedicine, energy-related applications, and environmental monitoring, each of those are supported by tables summarizing the main parameters of EC-SERS approach efficiency.

5.1. Biomedical applications

Biomedical applications, such as healthcare, laboratory diagnostics (*in vitro*), biochemistry, biotechnology, cell biology, and biological engineering, require detection methods that could achieve and even overcome *clinically relevant levels of sensitivity*, *quantification of the concentrations*, and *high specificity* with low false positive and false negative rates. The range of works reviewed below shows that EC-SERS detection fulfills all these requirements. In Table 2 we also show the main quantitative and qualitative indicators achieved by now to highlight how promising EC-SERS is in biomedicine.

Gu et al.[137] demonstrated the extremely low LOD of 0.3 and 0.6 pg mL^{-1} for two cancer biomarkers, carcinoembryonic antigen (CEA) and *alpha*-fetoprotein, respectively, using a gold microarray electrode immunoassay platform for simultaneous dual EC and SERS readouts. In addition, this sensor was used to detect serum in human blood, collecting the probes from both healthy and sick people. The performance is comparable with the existing clinical methods, with a recovery ranging from 95 to 107,5%. The improved sensitivity and quantification of the analyte were shown by Zhou et al.[138] for miRNA detection (Figure 4a). The authors achieved incredibly low LODs of 0.12 fM for SERS and 2.2 fM for EC. First of all, the 3 D popcorn-like Au NP film electrodes with a high ECSA contributed to the signal enhancement; secondly, the toehold-mediated strand displacement amplification reaction improved the signal-to-noise ratio; finally, the dual-channel detection itself contributed to higher accuracy. Another impressive work by Ilkhani et al.[139] showed for the first time the ability of the chemotherapeutic drug doxorubicin to intercalate DNA molecules (Figure 4b). The remarkable specificity of SERS allowed tracing the drug intercalation in DNA, whereas EC measurements provided dose-dependent information. The proposed approach can be considered a relatively inexpensive and straightforward way to test new drugs at their development stage.

The high specificity of EC-SERS was also shown for the case of bacterial detection. For SERS alone, identification remains controversial due to the complex signals and relatively low signal enhancement with such large objects. Do and colleagues have shown an EC-SERS sensor to determine bacteria toxin pyocyanin in biofilms as an early infection marker under different pH and electrical potentials.[140] The EC-SERS approach is beneficial since the bacteria secretion complex includes different small molecules, which are Raman and redox-active. The EC-SERS demonstration in liquid conditions makes it attractive for analyzing bacteria biofilm formation in water pipes and containers for early measures to minimize infection spread. The synergy of EC-SERS appears not only in improved detection sensitivity but also in distinguishing between *E. coli* K-12 and *B. megaterium* by the group of Brosseau, one of the leading groups in

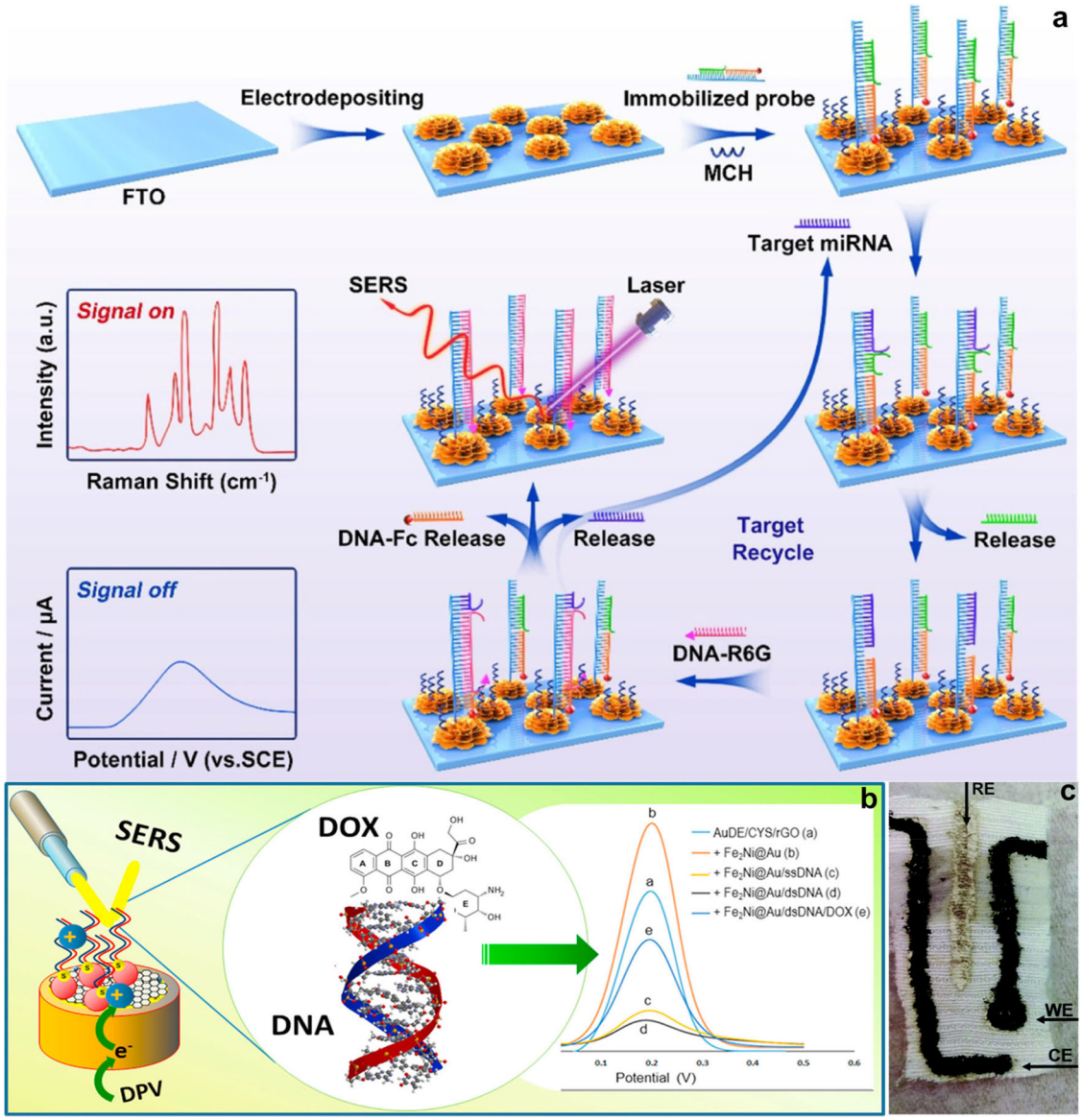

Figure 4. a) Schematic Illustration of the Proposed Strategy for Enzyme-Free Target Recycling Amplification Detection of miRNA. Adapted with permission from Ref. [138] Copyright (2021) American Chemical Society; b) Scheme of the self-assembled monolayer protected gold-disk electrode (AuDE) was coated with a reduced graphene oxide (rGO), decorated with plasmonic gold-coated Fe2Ni@Au magnetic nanoparticles functionalized with double-stranded DNA (dsDNA), a sequence of the breast cancer gene BRCA1 (AuDE/SAM/rGO/Fe2Ni@Au/dsDNA) nanobiosensor working principle for EC-SERS transduction, enabling chemically specific and highly sensitive analytical signals generation;[139] c) A photograph of the fabric-based sensor, the configuration contains three electrodes (WE, CE, RE).[104]

portable EC-SERS.[4] They analyzed seven nucleotide breakdown products of bacteria and studied each component's proportion at an electrode potential of −1 V that allowed strain identification.[141] For the first time, bacteria screening and discrimination were possible with the EC-SERS approach.

To achieve such record sensitivity and selectivity for bio-objects detection, the choice of the electrode material is of high importance: its effect on the bio-object stability must be taken into account. In this case, existing options for WE vary from commercial carbon SPE to paper or textiles [98,104] modified with a range of materials from Au or Ag NPs [95] to more complex materials with multimetal NPs[4] [] or NPs of specific shapes.[94,138] By combining the EC-SERS electrodes with specific biofunctionalization approaches, such as using antibodies or aptamers, it is possible to obtain an almost unlimited range of test system designs for various bioanalytical purposes.[94,137–139,143–145] Such a technique has been implemented in an immunosensor to detect CEA, a tumor biomarker, by sequential measurements with EIS and SERS at physiologically relevant concentrations with high accuracy[94] (Figure 4).

The critical challenge in biomedical analysis is developing point-of-care methods. Using the EC-SERS approach with an additional set of functionalized SERS electrodes could be potentially a universal analytical point-of-care platform with clinically relevant screening parameters. Such methods would rely on easily analyzing collectable biological liquids such as urine and saliva but have to overcome the challenge of complex spectral response both in EC and SERS. The combined approach was successfully applied to detect tuberculosis DNA and common antibiotic levofloxacin in synthetic urine.[104,144] A bimetallic EC-SERS substrate was proposed by Zhao et al.[142] and employed to detect uric

acid, a potential biomarker of preeclampsia, in synthetic urine in clinically relevant concentrations. Portable EC-SERS setup recently showed its applicability for evaluating the effectiveness of immunosuppression therapy for cancer patients. It has been successfully used to detect 6-thiouric acid (6-TUA) at μM levels in synthetic urine. 6-TUA is a metabolite of the immunosuppressive drug azathioprine, commonly used for bone marrow transplants.[146] Thus, the portable versions of EC and SERS, and EC-SERS electrode functionalization techniques prove that this combination is universal and valuable enough for point-of-care diagnosis. However, in that work, authors used synthetic urine as the analyte, with a perspective to take biomaterial from real patients in future clinical studies. As for saliva analysis, Velicka et al.[147] showed the detection of caffeine and its metabolite paraxanthine in human saliva samples using a WE decorated with Ag NPs (Table 2).

These examples demonstrate that EC-SERS is promising to become an efficient tool for noninvasive diagnosis of pathological conditions, monitoring patient status and therapy effectiveness, and is suitable for point-of-care applications.[104] An interesting strategy may be the development of textile-based EC-SERS sensors that could be upgraded for wearable EC-SERS-based analytic systems (Figure 4c).[104] The EC-SERS coupling was implemented for drug detection,[98,147–149] biomolecule analysis,[94,95,137,138,142–144,150,151] and bacteria detection [141] to improve the limit of detection, sensitivity, and accuracy that would make it genuinely competitive in comparison to existing analytical approaches. In addition, the EC-SERS benefits from various functionalizations developed to detect specific biomolecules that make it versatile and highly specific.

5.2. Photocatalysis and energy applications

5.2.1. Relevance in photocatalysis and energy-related research

Energy storage and generation is a hot topic for the global community nowadays to prevent the energy crisis and reduce environmental pollution.[152] Meanwhile, the core of modern energy solutions is chemical reactions. The most crucial of them include hydrogen evolution reaction (HER), a cathodic reaction in electrochemical water splitting to obtain high-purity hydrogen. Oxygen evolution and reduction reactions (OER and ORR) are used in batteries and fuel cells. Finally, a CO_2 reduction reaction (CO_2RR) is employed to gather the energy released during the reaction while at the same time reducing CO_2 concentration to mitigate the greenhouse effect. The low efficiency and control of these reaction pathways and products remain challenging. Catalysis is the key to reducing the activation energy of the energetically demanding chemical reactions and improving selectivity. (Photo)catalysis, in particular, has a significant impact on the energy industry due to various possible applications such as energy storage, harvesting, environmental conservation, and others, providing clean and renewable energy sources.[153–155] In this regard, investigating

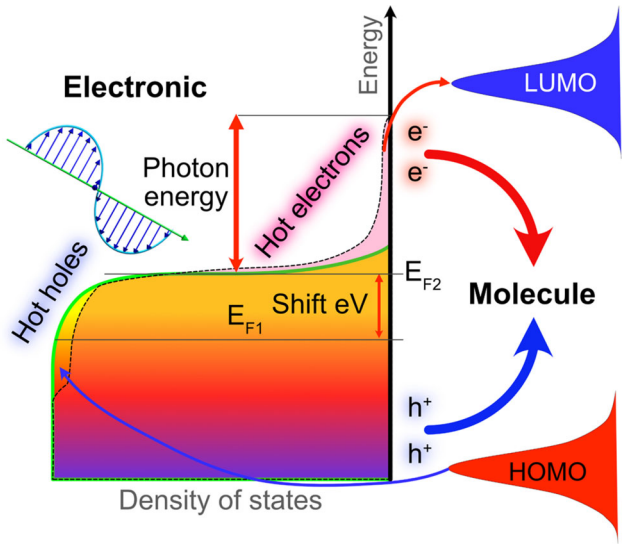

Figure 5. Electronic band diagram of energy levels in plasmon-induced photocatalysis.

(photo)catalysis mechanisms and developing effective (photo)catalysts is an important challenge.

In order to catalyze chemical reactions, an effective way is to use various plasmonic nanostructures.[156–159] Since plasmonic nanostructures are also necessary for SERS detection, EC-SERS is uniquely suitable for investigating such reactions' fundamental mechanisms and energy-related variations. In plasmon-induced photocatalysis, the metal nanostructures can inject highly energetic electrons (or holes) into a molecule in close contact, resulting in a photocatalytic reaction (Figure 4). Although this name may be misleading, these highly energetic electrons are also called "hot electrons."[160] Hot electrons originate from the non-equilibrium distribution of conduction electrons in the plasmonic NPs that results in electrons (holes) occupying higher (lower) energy levels than set by the Fermi distribution at room temperature.[161] Thus, such energetic electrons (holes) can be transferred more easily to the LUMO, HOMO of a molecule in contact with the plasmonic NPs (Figure 5).[162] However, in addition to this charge-transfer mechanism to explain plasmon-induced photocatalysis, the local temperature increase in the plasmonic NPs under resonance light excitation can also contribute to the photocatalytic transformation[163–165] (Figure 5).

The implications of EC-SERS in energy-related research could vary from the simple characterization of ions, like in dehydrogenase catalysis,[166] to the vital tool for *in situ* analysis of the catalytic reactions as it can provide real-time spectroscopic information on how electrochemical reactions occur. That is relevant as some reactions cannot be induced only with light, and electrochemistry comes into play here. SPR could drive several heterogeneous catalytic reactions, even though their performance could be significantly improved by applying electrical potential. The typical model systems for studying photocatalytic reactions are thiols.

For instance, in SERS of thioanisole, there are potential-dependent Raman peaks at 464 cm^{-1} and 1584 cm^{-1} that are attributed to the S-S bond indicating dimerization and benzenyl group stretching respectively and occur only

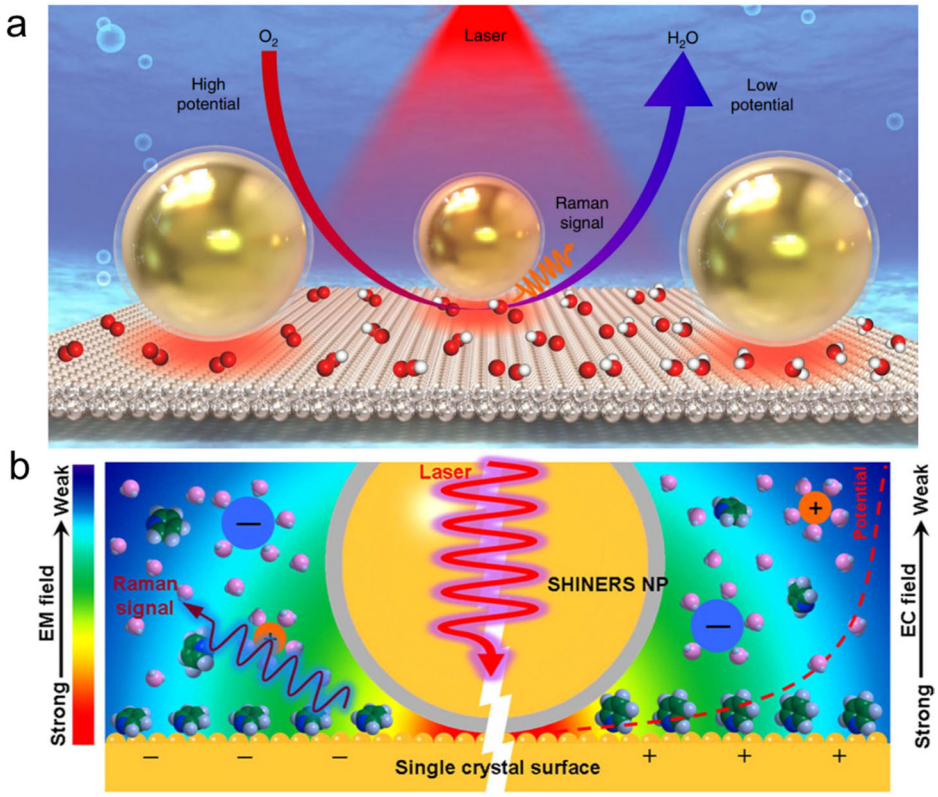

Figure 6. a) Schematic diagram of EC-SHINERS. The coexistence of electromagnetic (EM) and electrochemical (EC) fields is shown, with the electrode surface more negative at the left and more positive at the right Adapted with permission from Ref. [187]. Copyright 2015 American Chemical Society, b) Model of the shell-isolated NPs (Au@SiO2 NPs, SHINs) at a Pt(111) surface and the mechanism of the ORR process revealed by the EC-SHINERS method.[185]

starting from the potential of −0.4 V vs. Ag/AgCl RE at an electrochemical cell which contained a 0.1 M KCl solution. The Raman modes' intensity and their splitting occur with further potential increase.[112] These findings are essential to proposing the mechanisms of a surface chemical reaction, starting from the barrier of dimerization. Another example is a dehydroxylation reaction to produce thiophenol achieved during the SERS investigation of *p*-hydroxythiophenol on the surface of roughened silver as a model system for heterogeneous catalytic reactions. The reaction only occurs when applying the potential and goes faster in acidic solutions.[167]

EC-SERS could drive some reactions selectively, like in the case of 4-ABT transition to DMAB on the surface of roughened silver in 0.1 M $NaClO_4$. During the illumination with a high-power laser, 4-ABT molecules are oxidized to DMAB, while DMAB can be reduced to 4-ABT at negative potentials with a complete reduction at the potential of about −0.8 V at the Ag electrode. Therefore, laser leads to the formation of DMAB, while electrochemical reduction converts it back to 4-ABT.[168] Three main factors affect plasmon-driven chemical reactions: surface plasmons, plasmon resonance, and applied potential, whose increase makes it possible to overcome the junction barrier more easily. It is especially relevant to a potential-dependent, plasmon-driven catalytic reduction reaction of 4,4′-dinitroazobenzene (DNAB) nitro group (NO_2) to amine group (NH_2). EC-SERS spectra were measured in an electrochemical cell containing a solution of 0.1 M Na_2SO_4 at potentials from 0 to −1.2 V, and DNAB occurs between −0.8 and −0.9 V with 532 nm laser excitation. Meanwhile, for 4-nitro-4′-aminoazobenzene, the reaction is observed even at 0 V, which means that reaction has a much lower barrier.[169]

The photocatalytic reactions driven by charge transfer could also be suppressed by using ultrathin silica or alumina shells on gold NPs such as those used in SHINERS. This way, NPs are not in direct contact with a molecule that undergoes reaction upon the charge transfer, while the SERS effect could be achieved since it relies on the electromagnetic enhancement that extends beyond the silica shell.[170]

5.2.2. Specific reactions studied for energy conversion applications

The HER, OER, ORR, and CO_2RR catalytic reaction mechanisms were investigated using the combination of electrochemical and optical methods and are discussed in this section.

Recently, the SERS platform was demonstrated to study electrochemical HER mechanisms using MoS_2.[171] MoS_2 was suggested as a low-cost alternative catalyst for electrochemical hydrogen production from water.[172–174] Chen et al., obtained Ag core-shell heterostructure ($Ag@MoS_2$) that demonstrates the size-dependent electrochemical activity toward HER. $Ag@MoS_2$ core − shell heterostructures were obtained via a two-step wet-chemical synthesis by the chemical transformation of $Ag_2S@MoS_2$. First, to initiate the growth of MoS_2 on the surface of Ag_2S nanocrystals, Mo-oleylamine (OM) stock solution was injected. The mixture was then cooled down with the further addition of S_2

Table 3. EC-SERS sensors in Photocatalysis and Energy Applications.

Analyte	Substrate (WE)	Functionalization	Potential at which the reaction begins to occur	RSTD/reproducibility	Efficiency and important observations	Time of analysis	Reference
TP	Roughened Ag	PHTP	−0.3 V	–	Maximum TP/PHTP intensity ratios: 1.29 (pH 2), 1.71 (Power 20 mW), 1.81 (Wavelength 532 nm)	–	[167]
PATP	Roughened Ag	DMAB	−0.6 V	–	The intensities of the 1140, 1388, and 1438 cm^{-1} bands dramatically changed with the potential shift from −0.6 to −1 V	90 s	[168]
DMAB	Roughened Ag	4NTA	−0.4 V	–	From −0.6 to −1.2 V, the Raman peaks at 464, 1573/1585 cm^{-1} gradually increase as the thiophenol dimer is formed. The dimerization is stable.	–	[112]
Hydrogen	Ag@MoS_2 heterostructure	MoS_2	−250 mV	>10000 cycles	Highest signal (combination of HER activity and SERS) was obtained on the Ag@MoS_2 with a size of 23.4 ± 3.8 nm	–	[171]
Oxygen	Roughened Au	–	1.4 V	–	Surface-bound OOH was observed on an Au anode. Au-OOH species are the precursors to O_2 in OER. 815–830 cm^{-1} band originates only from OOH species formed during OER	3 s for each spectra	[176]
Oxygen	Au@SiO_2	Pt_3Co	0.7 V	–	Bridge adsorbed oxygen (b-O_2*) and *OOH (bands at 711 and 876 cm^{-1}) at Pt sites detected in acidic and basic solutions. Adsorbed *OH (band at 756 cm^{-1}) detected at Co sites in basic solution. Weaker interactions between Pt and adsorbed intermediates (O*) lead to improved ORR activity	–	[203]

TP, thiophenol; PHTP, p-hydroxythiophenol; DMAB, 4,4′-dimercaptoazobenzene; PATP, p-aminothiophenol; 4NTA, 4-nitrothioanisole; HER, hydrogen evolution reaction; OER, oxygen evolution reaction; ORR, oxygen reduction reaction.

ethanol. Next, Ag_2S@MoS_2 was added to OM. The slurry was degassed and heated. The mixture was then purged with nitrogen and heated. Right after, trioctylphosphine was injected into the solution. Finally, after being kept at 150 °C for 5 min, the Ag@MoS_2 mixture was cooled down and collected. EC-SERS was performed to study the HER process on the single-layer MoS_2-coated polyhedral Ag@MoS_2 heterostructure. Based on the obtained spectral evidence of S-H-bond formation, it was possible to suggest that the S atom in MoS_2 is the catalytically active center of HER. The highest SERS signal was obtained during electrochemical HER on the Ag@MoS_2 with a heterostructure size of 23.4 ± 3.8 nm.[171]

The SERS study of widely used iron porphyrin electrocatalysts, being widely used for ORR in aqueous solutions, was performed directly on a rotating disk electrode. Spectroscopic and electrochemical data are required to investigate the intermediates occurring during electrocatalysis, their nature, and the catalysis mechanism. Such a combination of dynamic electrochemistry with SERS was successfully applied at different potentials corresponding to the ORR conditions to understand the role of various axial ligands in the mechanism of electrochemical oxygen reduction *in situ*.[175] The issues of water electrochemical splitting, such as low OER efficiency and activity, are associated with the overpotential in anodic OERs, which is why this reaction mechanism is essential to understand. EC-SERS allows investigating the anodic OER and illustrating the presence of OOH species as intermediates in the SERS spectra during the OER, which is not possible to confirm using solely electrochemical methods. In the case of Au surfaces, the proposed mechanism is oxygen coupling on the Au surface to produce surface-bound -OOH at potentials where O_2 is released from the electrode surface for the electrochemical evolution of O_2 on the Au anode. These findings are in agreement with the theoretical studies and could significantly contribute to understanding the elementary processes involved in the electrochemical oxidation of water.[176]

Considering the advancements in the investigation of ORR reaction mechanisms, a notable review, which demonstrates advancements in probing the oxygen electrochemistry with *in situ* SERS, was recently published.[177] Wang et al. summarized recent progress in developing and monitoring Li-O_2 batteries in Li^+-induced ORR catalytic systems. SERS

Table 4. EC-SERS sensors in Environmental Applications.

Analyte	Substrate (WE)	Functionalization	LOD	Analytical range	RSTD/reproducibility	Selectivity	Time of analysis	Ref.	Comments
CBZ	Ti2C MXene/ Au–Ag NSs nanohybrid	–	SERS: 10^{-1} M EC: 2×10^{-1} M	SERS: 0.033–10 μM (with respect to 964 cm^{-1}) EC: 0.006–9.8 μM	SERS: 2.8% EC: 1.41% (for 30 cycles om a single electrode); 2.77% (current response between 13 electrodes	–	–	[190]	
Chlorfenapyr	AgNPs: glucose test strip	–	SERS: 7 ppm EC: 4.2 ppm	EC: 20–50 ppm	SERS: 17.6% (between 10 spots at the same sample) 30.3% (between 10 samples) EC: average 22%, but below 20% for concentrations higher than 30 ppm (for different samples	Selectivity was tested by mixing with ICD and triadimefon SERS: characteristic peak in not affected EC: characteristic peaks are visible and shift is only 2.20% (in presence of ICD) and 1.19% (in presence of triadimefon)	–	[193]	
Pb(II)	Golden disk electrode with EC deposited AuNPs	AB18C6	SERS: 6.9×10^{-13} M	SERS: 1 pM–1 μM	SERS: signal intensity was same for 7 samples	Selective toward Pb(II) over 10 other metals ions	–	[194]	EC wa used for substrate recovery via desorption of Pb(II)
Hg^{+}	Nanoporous gold	Poly(thymine)-based aptamer	SERS: 0.1 pM	SERS: up to 10 μM	SERS: deviation of signal intensity 5%–8% over 7 cycles	Change in intensity around 15% in presence of 13 other ions	–	[101]	Indirect detection (decay of signal intensity from aptamer in presence of Hg^{+}) To increase sensitivity potential was applied
Paracetamol	Gold capped glass nanopillars	–	–	EC: 30 μM–3 mM	SERS: Spatial uniformity of enhancement factor RSTD 13%	–	–	[96]	–

CBZ, carbendazim; NS, nanoshuttle; AB18C6, 4-amino-benzo-18-crown-6.

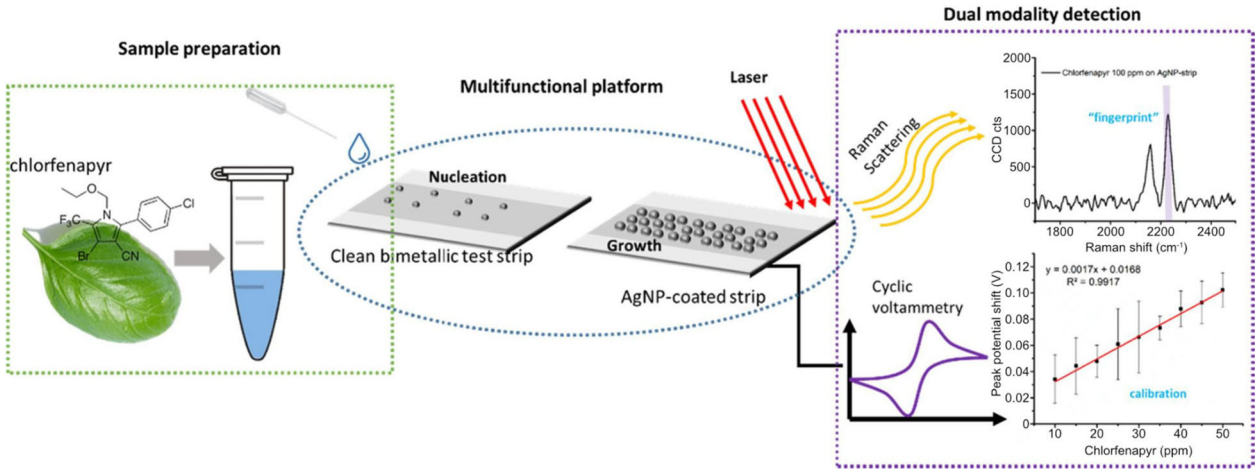

Figure 7. Schematic of multimodal sensors combining different detection methodologies on a single platform for dual functional detection of chlorfenapyr via EC-SERS.[193]

allows the acquisition of spatial and chemical information in oxygen electrochemical reaction mechanisms. The authors discussed different strategies to overcome the *in situ* SERS limitation of only a few compatible substrates (Au, Ag, and Cu). One of the solutions is the use of SHINERS. The Raman signal can be amplified with isolated Au NPs (coated with ultra-thin SiO_2 with no pinholes) and used as an effective alternative for SERS inactive substrates. In addition, it was reported that SERS and *in situ* SERS had been used to investigate other battery mechanisms, including complex electrode deposition/decomposition behavior.[178–183] For instance, EC-SHINERS was applied to investigate ORR, essential for fuel cells and batteries, on Pt_3Co nanocatalysts. *In situ* EC-SHINERS was performed in an O_2-saturated solution from 1.1 V to 0.2 V versus the reversible hydrogen electrode and allowed for detection of bridge adsorbed oxygen (b-O_2*), and *OOH reaction intermediates at Pt sites, and adsorbed *OH at Co.[184] EC-SHINERS was also used to systematically investigate the ORR process at Pt single-crystal surfaces to obtain direct spectral evidence of OH*, HO_2*, and O^{2-} (Figure 6a).[185] In the above-mentioned cases, SHINERS is applied to learn the electrochemical mechanisms and processes taking place in ORR reactions. SHINERS itself does not directly contribute to EC but makes it possible to see some spectral evidence that is hidden without the use of this approach.

Using EC-SERS for CO_2RR investigation is attractive as EC helps to study electron transfer, while SERS gives *in situ* information of oxidized and reduced species with plasmonic nano-gaps. That could be useful in renewable fuels, as was demonstrated for a nickel bis(terpyridine) complex sandwiched by thiol-anchoring moieties between two gold surfaces.[186] The experiments allowed tracking the redox transitions of eight molecules providing information on single-molecule catalysts. Moreover, for the catalytic mechanism investigation, EC-SERS could be coupled with theoretical studies with the help of density functional theory calculations (Figure 6).

Overall, the molecular-level understanding of ORR, HER, OER, and CO_2RR is essential for the rational design of highly active catalysts for energy applications. EC-SERS, especially *in situ* EC-SHINERS, proved to be an efficient method for characterizing materials and interfaces in various electrochemical systems, especially on the surface of single-crystal electrodes (Figure 6b).[187] To provide a more detailed analysis of the discussed works regarding materials, functionalization, efficiency, important observations etc., we made a summary in Table 3.

5.3. EC-SERS in environmental applications

The rapid growth of pollution levels caused by industrialization and the constant rise in produced waste results in a challenge to detect harmful compounds, such as heavy metals, toxic chemicals, pesticides, dyes, and pharmaceutical residuals (available quantitative values and achievements could be found in Table 4).[188,189]

On the one hand, the EC part offers chemical detection with low detection limits, aided by electrochemical transformations, while the light used in SERS promotes sensitivity and plasmon-induced photocatalytic decomposition of pollutants. On the other hand, the byproducts can be detected or transformed during the EC-SERS measurements, contributing to the detection by either method. Therefore, EC-SERS dramatically decreases the chances of a pollutant going undetected compared to conventional methods such as coagulation and adsorption. For example, if a pollutant redox potential is beyond the electrochemical window of the EC system, then at least EC could be used to maximize the SERS detection *via* a tuning enhancement mechanism. At the same time, the charge transfer and plasmon photocatalysis of the pollutant could produce species that fall within the EC window, allowing the detection of products using the EC channel.

The equivalent combination (Table 1) was recently implemented for ultrasensitive detection of carbendazim, a widely used pesticide, in rice and tea. For that purpose, graphene-like titanium carbide MXene/Au-Ag nanoshuttles were combined with machine learning for both EC and SERS. Mutual verification contributed to enhancing the sensitivity of carbendazim detection.[190] Another example is trinitrotoluene

(TNT) detection. TNT is an explosive and toxic compound widely used in manufacturing; its residues pollute the air, water, soil, and biosphere. TNT has low optical absorption, but it becomes optically visible due to the reaction with amine complexes.[191,192] Another dual-functional EC-SERS sensor was developed by Sanger et al. using silica nanostructures with Au nanowires deposition to form SPE-shaped electrodes. The sensor showed high electrocatalytic activity to paracetamol with the oxidation potential of 300 mW, and allowed its quantitative detection.[96] Moreover, remarkable LODs of 4.2 ppm using EC and 7 ppm using SERS were recently achieved with the complementary EC-SERS detection of chlorfenapyr, agricultural insecticide, and a toxin. SERS was used for the analyte identification, while qualitative analysis was done with a contribution of EC (Figure 7).[193]

The combination of Raman spectroscopy with plasmonics recently impacted portable water pollutants detection.[194] A novel sensor developed by Sarfo et al. has shown an excellent selectivity for Pb^{2+} ions. The LOD and limit of quantification (LOQ) were extremely low (0.69 pM and 2.20 pM, respectively). This SERS sensor has also been successfully used to detect lead ions in drinking water while capable of dealing with matrix effects. EC, in this case, was used for the treatment of SERS substrate for repeated SERS detection of Pb(II) ions. In particular, the aminobenzo-18-crown-6 with Pb(II) ions (AB18C6-P(II)) complex was desorbed from the substrate surface by cyclic voltammetry. After that, SERS was used to confirm the removal of AB18C6-P(II). Then, the AB18C6-P(II) complex was deposited and obtained SERS spectra, demonstrating that electrochemical treatment did not compromise the SERS activity. Exploiting the electrostatic potential to concentrate Hg^{2+} ions for SERS detection was also shown by Zheng et al., who achieved an impressive sub-picomolar detection limit.[101] Another example was reported by Kandjani et al., who exploited the plasmonic properties of Ag/ZnO arrays to detect and remove mercury ions from wastewater.[195] While the plasmonic electromagnetic field enhancement was used in conventional SERS detection of Hg^{2+}, the plasmon-induced charge transfer resulted in the reduction of Hg^{2+} to metallic mercury that was then removed by annealing at 150 °C. Dyes decolorization and detoxification are of high importance for water treatment as well. Thus, EC and SERS organic pollutants degradation efficiency comparison and their joint implementation were demonstrated to decompose azo dyes.[196] The potential-dependent spectra indicated that dye reduction in an aqueous solution is a multi-step process with the electrochemical reduction onset potential at −0.5 V with Ag/AgCl/KCl electrode in 0.1 mol L^{-1} KCl solution (Table 4).

To summarize, EC-SERS is proven to be a superior analytical approach for environmental applications. In the future, plasmon photocatalysis can offer considerable benefits in water remediation since it could allow harvesting sunlight to decompose pollutants into less harmful products or those that could be more easily removed.

6. Conclusions

Several reasons make a combination of EC methods with SERS a powerful analytical approach. Using independent detection channels, EC and SERS could give complementary information and cover the blind spots of each other, reducing the risk of false results. Experimentally, the EC electrode and SERS substrate can be realized as a single SERS electrode—a conductive surface with plasmonic activity fabricated from Au or Ag nanoparticles or films with the surface functionalization for targeting specific analytes. Both methods impose similar requirements for the sample preparation and SERS electrodes, like a high surface area. It makes their work together almost straightforward. However, EC requires an electrolyte medium to operate. SERS can be performed in different environments from air and liquid to a controlled atmosphere, so it poses little problem for both methods to work together.

While new developments such as SERS and TERS boosted Raman spectroscopy, conventional EC reached its limits a while ago. Thus, EC is benefiting a lot from this combination. However, a closer look into increasing SERS signals by applying electrical potential shows that SERS also has much to gain from EC. Compared to the conventional Raman technique, SERS can reach remarkable sensitivity. However, many strategies are being developed to drive SERS sensitivity even further. These strategies are based on preconcentration, either with magnetic fields or with hydrophilic/hydrophobic interactions. EC can also serve as a preconcentration method for SERS by exploiting the electrostatic interaction between the analyte and the working (SERS) electrode. Moreover, in contrast to magnetic and hydrophobic/hydrophilic pre-concentration, EC is readily tunable and reversible.

SERS techniques coupled with electrochemical methods provide a powerful tool with some limitations for investigating and characterizing various target molecules. Different setups are used depending on the analyte and the EC-SERS combination types. In biomedical applications, dual readout demonstrates high sensitivity with clinically comparable LOD, potentially expanding the *point-of-care* clinical toolkit. Although LOD and sensitivity of EC-SERS are competitive, it is still not enough to overcome the existing clinical methods. Comparing EC-SERS with existing clinical approaches such as enzyme-linked immunosorbent assay (ELISA), LC-MS/MS, PCR, electrophoresis, chemiluminescence immunoassay (CLIA), etc. several areas of its improvement could be identified. They include analysis time, cost-effectiveness, throughput, process automatization, and standardization of all analysis steps. Improvement of these parameters will allow EC-SERS to be one of the top analytical techniques for clinical implementation.

EC-SERS is highly beneficial for studying plasmon-induced reactions and tuning their reactivity by applying bias. Investigation of HER, OER, ORR catalytic reactions with EC-SERS(SHINERS) methods allows the acquisition of chemical and spatial information. Therefore, a deeper understanding of catalytic mechanisms could be obtained and used to develop novel energy storage and harvesting

systems. However, the spatial and temporal resolution of EC-SERS methods still needs to be improved in the future.

EC-SERS also contributes to detecting environmental pollutants with an improved sensitivity, which is critical for food analysis, water remediation, and environmental monitoring.

7. Outlook

While the EC-SERS combination has some powerful benefits, a few drawbacks are also worth considering. For instance, SERS requires conductive and plasmonic materials. These materials pose some complications when analyzing biomolecules due to the strong biomolecule/metal interaction that could induce, for example, conformation changes of proteins. This challenge is well-known in the EC community, and, therefore, other electrode materials, such as glassy carbon, are preferable instead of gold. However, for SERS, glassy carbon cannot be suitable since its conduction electrons have no plasmon resonances in the visible spectral range, and therefore are not SERS active with conventional Raman spectrometers. Thus, SERS requires WE to contain plasmonic NPs, but it poses a risk of molecule decomposition. This challenge can be addressed by developing nonmetallic SERS substrates, which have been gaining momentum in recent years.

One of the most exciting applications of EC-SERS is that it allows mimicking the electrostatic conditions of living systems. This is highly promising for understanding the mechanism and function of different molecules and cell components from the mitochondria to the cell membrane and the interaction of different cell types with various drugs, which is paramount for pharmaceutics and healthcare. Also, the first portable and field-deployable devices are expected to appear in the near future. Portable EC and SERS units already exist and could be integrated into some smart devices such as laptops or smartphones, making it possible to use the EC-SERS sensor in the field conditions, which in turn will massively expand scenarios of EC-SERS setup applications[120,146,197].

Moreover, SERS allows the investigation of cells and other biomaterials' interactions with different electrode materials. For example, protein unfolding or denaturation in the process of interaction with the WE could be evidenced with SERS simultaneously such that the changes observed in a cyclic voltammetry experiment could be appropriately assigned not only to redox properties but also to structural changes.

Declaration of competing interest

The authors declare that they have no known competing financial interests or personal relationships that could have appeared to influence the work reported in this paper.

Funding

The reported study was funded by RFBR and DFG, project number 21-53-12045, DFG project no. KA 1663/13-1.

References

[1] Ma, C.; Cao, Y.; Gou, X.; Zhu, J.-J. Recent Progress in Electrochemiluminescence Sensing and Imaging. *Anal. Chem.* **2020**, *92*, 431–454. DOI: 10.1021/acs.analchem.9b04947.

[2] Ronspees, A. T.; Thorgaard, S. N. Blocking Electrochemical Collisions of Single E. Coli and B. Subtilis Bacteria at Ultramicroelectrodes Elucidated Using Simultaneous Fluorescence Microscopy. *Electrochim. Acta* **2018**, *278*, 412–420. DOI: 10.1016/j.electacta.2018.05.006.

[3] Yuan, T.; Wang, W. Studying the Electrochemistry of Single Nanoparticles with Surface Plasmon Resonance Microscopy. *Curr. Opin. Electrochem.* **2017**, *6*, 17–22. DOI: 10.1016/j.coelec.2017.06.009.

[4] Lynk, T. P.; Sit, C. S.; Brosseau, C. L. Electrochemical Surface-Enhanced Raman Spectroscopy as a Platform for Bacterial Detection and Identification. *Anal. Chem.* **2018**, *90*, 12639–12646. DOI: 10.1021/acs.analchem.8b02806.

[5] Chen, Z.; Jiang, S.; Kang, G.; Nguyen, D.; Schatz, G. C.; Van Duyne, R. P. Operando Characterization of Iron Phthalocyanine Deactivation during Oxygen Reduction Reaction Using Electrochemical Tip-Enhanced Raman Spectroscopy. *J. Am. Chem. Soc.* **2019**, *141*, 15684–15692. DOI: 10.1021/jacs.9b07979.

[6] Ji-Yang, J.-Y.; Dong, J.-C.; Vinod Kumar, V.; Li, J.-F.; Tian, Z.-Q. Probing Electrochemical Interfaces Using Shell-Isolated Nanoparticles-Enhanced Raman Spectroscopy. *Curr. Opin. Electrochem.* **2017**, *1*, 16–21. DOI: 10.1016/j.coelec.2016.12.009.

[7] Strange, L. E.; Yadav, J.; Garg, S.; Shinde, P. S.; Hill, J. W.; Hill, C. M.; Kung, P.; Pan, S. Investigating the Redox Properties of Two-Dimensional MoS2 Using Photoluminescence Spectroelectrochemistry and Scanning Electrochemical Cell Microscopy. *J. Phys. Chem. Lett.* **2020**, *11*, 3488–3494. DOI: 10.1021/acs.jpclett.0c00769.

[8] Jing, C.; Long, Y. Observing Electrochemistry on Single Plasmonic Nanoparticles. *Electrochem. Sci. Adv.* **2021**, *2021*, e2100115. DOI: 10.1002/elsa.202100115.

[9] Wang, Y.; Cao, Z.; Yang, Q.; Guo, W.; Su, B. Optical Methods for Studying Local Electrochemical Reactions with Spatial Resolution: A Critical Review. *Anal. Chim. Acta.* **2019**, *1074*, 1–15. DOI: 10.1016/j.aca.2019.02.053.

[10] Shi, Y.; Wang, J.; Wang, C.; Zhai, T.-T.; Bao, W.-J.; Xu, J.-J.; Xia, X.-H.; Chen, H.-Y. Hot Electron of Au Nanorods Activates the Electrocatalysis of Hydrogen Evolution on MoS2 Nanosheets. *J. Am. Chem. Soc.* **2015**, *137*, 7365–7370. DOI: 10.1021/jacs.5b01732.

[11] Zanut, A.; Fiorani, A.; Canola, S.; Saito, T.; Ziebart, N.; Rapino, S.; Rebeccani, S.; Barbon, A.; Irie, T.; Josel, H.-P.; et al. Insights into the Mechanism of Coreactant Electrochemiluminescence Facilitating Enhanced Bioanalytical Performance. *Nat. Commun.* **2020**, *11*, 2668. DOI: 10.1038/s41467-020-16476-2.

[12] Fleischmann, M.; Hendra, P. J.; McQuillan, A. J. Raman Spectra of Pyridine Adsorbed at a Silver Electrode. *Chem. Phys. Lett* **1974**, *26*, 163–166. DOI: 10.1016/0009-2614(74)85388-1.

[13] Lajevardi Esfahani, S.; Rouhani, S.; Ranjbar, Z. Layer-by-Layer Assembly of Electroactive Dye/LDHs Nanoplatelet Matrix Film for Advanced Dual Electro-Optical Sensing Applications. *Nanoscale Res. Lett.* **2020**, *15*, 210. DOI: 10.1186/s11671-020-03442-6.

[14] Martínez-Periñán, E.; Gutiérrez-Sánchez, C.; García-Mendiola, T.; Lorenzo, E. Electrochemiluminescence Biosensors Using Screen-Printed Electrodes. *Biosensors* **2020**, *10*, 118. DOI: 10.3390/bios10090118.

[15] Zhai, Y.; Zhu, Z.; Zhou, S.; Zhu, C.; Dong, S. Recent Advances in Spectroelectrochemistry. *Nanoscale* **2018**, *10*, 3089–3111. DOI: 10.1039/c7nr07803j.

[16] Wang, C.; Shi, Y.; Yang, D.-R.; Xia, X.-H. Combining Plasmonics and Electrochemistry at the Nanoscale. *Curr. Opin.*

Electrochem. **2018**, *7*, 95–102. DOI: 10.1016/j.coelec.2017.11.001.

[17] Eltzov, E.; Cosnier, S.; Marks, R. S. Biosensors Based on Combined Optical and Electrochemical Transduction for Molecular Diagnostics. *Expert Rev. Mol. Diagn.* **2011**, *11*, 533–546. DOI: 10.1586/erm.11.38.

[18] Juan-Colás, J.; Johnson, S.; Krauss, T. F. Dual-Mode Electro-Optical Techniques for Biosensing Applications: A Review. *Sensors* **2017**, *17*, 2047. DOI: 10.3390/s17092047.

[19] Moldovan, R.; Vereshchagina, E.; Milenko, K.; Iacob, B.-C.; Bodoki, A. E.; Falamas, A.; Tosa, N.; Muntean, C. M.; Farcău, C.; Bodoki, E. Review on Combining Surface-Enhanced Raman Spectroscopy and Electrochemistry for Analytical Applications. *Anal. Chim. Acta* **2021**, *2021*, 339250. noDOI: 10.1016/j.aca.2021.339250.

[20] Bandodkar, A. J.; Wang, J. Non-Invasive Wearable Electrochemical Sensors: A Review. *Trends Biotechnol.* **2014**, *32*, 363–371. DOI: 10.1016/j.tibtech.2014.04.005.

[21] Ahmad, Z. Corrosion Kinetics. In *Principles of Corrosion Engineering and Corrosion Control*; Elsevier: New York, NY, **2006**; pp 57–119.

[22] Job, R. *Electrochemical Energy Storage: Physics and Chemistry of Batteries*; De Gruyter: Berlin, Germany, **2020**. DOI: 10.1515/9783110484427.

[23] Mitra, C. K.; Prasad, M. N. V. Basic Electrochemistry Tools in Environmental Applications. In *Electrokinetic Remediation for Environmental Security and Sustainability*; Wiley: Hoboken, NJ, **2021**, pp 35–60. DOI: 10.1002/9781119670186.ch2.

[24] Wang, J. *Analytical Electrochemistry*, 3rd Ed.; Wiley: Hoboken, NJ, **2006**.

[25] Bard, A. J.; Faulkner, L. R.; White, H. S. *Electrochemical Methods: Fundamentals and Applications*; Wiley: Hoboken, NJ, **2022**.

[26] Zanello, P. *Inorganic Electrochemistry: Theory, Practice and Application*; Royal Society of Chemistry: London, UK, **2007**.

[27] Bansod, B.; Kumar, T.; Thakur, R.; Rana, S.; Singh, I. A Review on Various Electrochemical Techniques for Heavy Metal Ions Detection with Different Sensing Platforms. *Biosens. Bioelectron.* **2017**, *94*, 443–455. DOI: 10.1016/j.bios.2017.03.031.

[28] Kimmel, D. W.; LeBlanc, G.; Meschievitz, M. E.; Cliffel, D. E. Electrochemical Sensors and Biosensors. *Anal. Chem.* **2012**, *84*, 685–707. DOI: 10.1021/ac202878q.

[29] Ding, R.; Krikstolaityte, V.; Lisak, G. Inorganic Salt Modified Paper Substrates Utilized in Paper Based Microfluidic Sampling for Potentiometric Determination of Heavy Metals. *Sens. Actuators B Chem* **2019**, *290*, 347–356. DOI: 10.1016/j.snb.2019.03.079.

[30] Wang, H.; Yuan, B.; Yin, T.; Qin, W. Alternative Coulometric Signal Readout Based on a Solid-Contact Ion-Selective Electrode for Detection of Nitrate. *Anal. Chim. Acta.* **2020**, *1129*, 136–142. DOI: 10.1016/j.aca.2020.07.019.

[31] Nehru, R.; Hsu, Y.-F.; Wang, S.-F.; Dong, C.-D.; Govindasamy, M.; Habila, M. A.; AlMasoud, N. Graphene Oxide@Ce-Doped TiO Nanoparticles as Electrocatalyst Materials for Voltammetric Detection of Hazardous Methyl Parathion. *Mikrochim. Acta* **2021**, *188*, 216.

[32] Dabhade, A.; Jayaraman, S.; Paramasivan, B. Development of Glucose Oxidase-Chitosan Immobilized Paper Biosensor Using Screen-Printed Electrode for Amperometric Detection of Cr(VI) in Water. *3 Biotech* **2021**, *11*, 183. DOI: 10.1007/s13205-021-02736-5.

[33] Waheed, A.; Mansha, M.; Ullah, N. Nanomaterials-Based Electrochemical Detection of Heavy Metals in Water: Current Status, Challenges and Future Direction. *Trends Analyt. Chem* **2018**, *105*, 37–51. DOI: 10.1016/j.trac.2018.04.012.

[34] Kanoun, O.; Lazarević-Pašti, T.; Pašti, I.; Nasraoui, S.; Talbi, M.; Brahem, A.; Adiraju, A.; Sheremet, E.; Rodriguez, R. D.; Ben Ali, M.; et al. A Review of Nanocomposite-Modified Electrochemical Sensors for Water Quality Monitoring. *Sensors* **2021**, *21*, 4131. DOI: 10.3390/s21124131.

[35] Noori, J. S.; Mortensen, J.; Geto, A. Recent Development on the Electrochemical Detection of Selected Pesticides: A Focused Review. *Sensors* **2020**, *20*, 2221. DOI: 10.3390/s20082221.

[36] Ryu, H.; Thompson, D.; Huang, Y.; Li, B.; Lei, Y. Electrochemical Sensors for Nitrogen Species: A Review. *Sensors and Actuators Reports* **2020**, *2*, 100022. DOI: 10.1016/j.snr.2020.100022.

[37] Wang, B.; Akiba, U.; Anzai, J.-I. Recent Progress in Nanomaterial-Based Electrochemical Biosensors for Cancer Biomarkers: A Review. *Molecules* **2017**, *22*, 1048. DOI: 10.3390/molecules22071048.

[38] Khanmohammadi, A.; Aghaie, A.; Vahedi, E.; Qazvini, A.; Ghanei, M.; Afkhami, A.; Hajian, A.; Bagheri, H. Electrochemical Biosensors for the Detection of Lung Cancer Biomarkers: A Review. *Talanta* **2020**, *206*, 120251. DOI: 10.1016/j.talanta.2019.120251.

[39] de Eguilaz, M. R.; Cumba, L. R.; Forster, R. J. Electrochemical Detection of Viruses and Antibodies: A Mini Review. *Electrochem. Commun.* **2020**, *116*, 106762. DOI: 10.1016/j.elecom.2020.106762.

[40] Zribi, R.; Neri, G. Mo-Based Layered Nanostructures for the Electrochemical Sensing of Biomolecules. *Sensors* **2020**, *20*, 5404. DOI: 10.3390/s20185404.

[41] Hackethal, C.; Kopp, J. F.; Sarvan, I.; Schwerdtle, T.; Lindtner, O. Total Arsenic and Water-Soluble Arsenic Species in Foods of the First German Total Diet Study (BfR MEAL Study). *Food Chem.* **2021**, *346*, 128913. DOI: 10.1016/j.foodchem.2020.128913.

[42] Draz, M. E.; Darwish, H. W.; Darwish, I. A.; Saad, A. S. Solid-State Potentiometric Sensor for the Rapid Assay of the Biologically Active Biogenic Amine (Tyramine) as a Marker of Food Spoilage. *Food Chem.* **2021**, *346*, 128911. DOI: 10.1016/j.foodchem.2020.128911.

[43] Bala, K.; Sharma, D.; Gupta, N. Carbon-Nanotube-Based Materials for Electrochemical Sensing of the Neurotransmitter Dopamine. *ChemElectroChem* **2019**, *6*, 274–288. DOI: 10.1002/celc.201801319.

[44] Manikandan, V. S.; Adhikari, B.; Chen, A. Nanomaterial Based Electrochemical Sensors for the Safety and Quality Control of Food and Beverages. *Analyst* **2018**, *143*, 4537–4554. DOI: 10.1039/c8an00497h.

[45] Zribi, R.; Maalej, R.; Messina, E.; Gillibert, R.; Donato, M. G.; Maragò, O. M.; Gucciardi, P. G.; Leonardi, S. G.; Neri, G. Exfoliated 2D-MoS2 Nanosheets on Carbon and Gold Screen Printed Electrodes for Enzyme-Free Electrochemical Sensing of Tyrosine. *Sens. Actuators B Chem* **2020**, *303*, (127229. DOI: 10.1016/j.snb.2019.127229.

[46] Liu, X.; Chen, W.; Lian, M.; Chen, X.; Lu, Y.; Yang, W. Enzyme Immobilization on ZIF-67/MWCNT Composite Engenders High Sensitivity Electrochemical Sensing. *J. Electroanal. Chem* **2019**, *833*, 505–511. DOI: 10.1016/j.jelechem.2018.12.027.

[47] George, J. M.; Antony, A.; Mathew, B. Metal Oxide Nanoparticles in Electrochemical Sensing and Biosensing: A Review. *Mikrochim. Acta.* **2018**, *185*, 358.

[48] Vanova, V.; Mitrevska, K.; Milosavljevic, V.; Hynek, D.; Richtera, L.; Adam, V. Peptide-Based Electrochemical Biosensors Utilized for Protein Detection. *Biosens. Bioelectron.* **2021**, *180*, 113087. DOI: 10.1016/j.bios.2021.113087.

[49] Wang, A.; You, X.; Liu, H.; Zhou, J.; Chen, Y.; Zhang, C.; Ma, K.; Liu, Y.; Ding, P.; Qi, Y.; et al. Development of a Label Free Electrochemical Sensor Based on a Sensitive Monoclonal Antibody for the Detection of Tiamulin. *Food Chem.* **2022**, *366*, 130573. DOI: 10.1016/j.foodchem.2021.130573.

[50] Rebelo, P.; Costa-Rama, E.; Seguro, I.; Pacheco, J. G.; Nouws, H. P. A.; Cordeiro, M. N. D.; Delerue-Matos, C. Molecularly Imprinted Polymer-Based Electrochemical Sensors for

Environmental Analysis. *Biosens. Bioelectron.* **2021**, *172*, 112719. DOI: 10.1016/j.bios.2020.112719.
[51] Maduraiveeran, G.; Jin, W. Nanomaterials Based Electrochemical Sensor and Biosensor Platforms for Environmental Applications. *Trends Environ. Anal. Chem.* **2017**, *13*, 10–23. DOI: 10.1016/j.teac.2017.02.001.
[52] Zhang, Y.; Chen, X. Nanotechnology and Nanomaterial-Based No-Wash Electrochemical Biosensors: From Design to Application. *Nanoscale* **2019**, *11*, 19105–19118. DOI: 10.1039/c9nr05696c.
[53] Panjan, P.; Virtanen, V.; Sesay, A. M. Determination of Stability Characteristics for Electrochemical Biosensors via Thermally Accelerated Ageing. *Talanta* **2017**, *170*, 331–336. DOI: 10.1016/j.talanta.2017.04.011.
[54] Campuzano, S.; Pedrero, M.; Yáñez-Sedeño, P.; Pingarrón, J. Antifouling (Bio)Materials for Electrochemical (Bio)Sensing. *IJMS.* **2019**, *20*, 423. DOI: 10.3390/ijms20020423.
[55] Lin, P.-H.; Li, B.-R. Antifouling Strategies in Advanced Electrochemical Sensors and Biosensors. *Analyst* **2020**, *145*, 1110–1120. DOI: 10.1039/C9AN02017A.
[56] Tu, Q.; Chang, C. Diagnostic Applications of Raman Spectroscopy. *Nanomedicine* **2012**, *8*, 545–558. DOI: 10.1016/j.nano.2011.09.013.
[57] Das, R. S.; Agrawal, Y. K. Raman Spectroscopy: Recent Advancements, Techniques and Applications. *Vib. Spectrosc* **2011**, *57*, 163–176. DOI: 10.1016/j.vibspec.2011.08.003.
[58] Konorov, S. O.; Glover, C. H.; Piret, J. M.; Bryan, J.; Schulze, H. G.; Blades, M. W.; Turner, R. F. B. In Situ Analysis of Living Embryonic Stem Cells by Coherent anti-Stokes Raman Microscopy. *Anal. Chem.* **2007**, *79*, 7221–7225. DOI: 10.1021/ac070544k.
[59] Kudelski, A. Analytical Applications of Raman Spectroscopy. *Talanta* **2008**, *76*, 1–8. DOI: 10.1016/j.talanta.2008.02.042.
[60] McQuillan, A. J. The Discovery of Surface-Enhanced Raman Scattering. *Notes Rec. R Soc.* **2009**, *63*, 105–109. DOI: 10.1098/rsnr.2008.0032.
[61] Rodriguez, R. D.; Villagómez, C. J.; Khodadadi, A.; Kupfer, S.; Averkiev, A.; Dedelaite, L.; Tang, F.; Khaywah, M. Y.; Kolchuzhin, V.; Ramanavicius, A.; et al. Chemical Enhancement vs Molecule–Substrate Geometry in Plasmon-Enhanced Spectroscopy. *ACS Photonics* **2021**, *8*, 2243–2255. DOI: 10.1021/acsphotonics.1c00001.
[62] Le Ru, E. C.; Meyer, M.; Etchegoin, P. G. Proof of Single-Molecule Sensitivity in surface enhanced Raman Scattering (SERS) by Means of a Two-Analyte Technique. *J Phys Chem B* **2006**, *110*, 1944–1948. DOI: 10.1021/jp054732v.
[63] Zhou, H.; Yang, D.; Ivleva, N. P.; Mircescu, N. E.; Niessner, R.; Haisch, C. SERS Detection of Bacteria in Water by in Situ Coating with Ag Nanoparticles. *Anal. Chem.* **2014**, *86*, 1525–1533. DOI: 10.1021/ac402935p.
[64] Hou, R.; Pang, S.; He, L. In Situ SERS Detection of Multi-Class Insecticides on Plant Surfaces. *Anal. Methods* **2015**, *7*, 6325–6330. DOI: 10.1039/C5AY01058F.
[65] Xiong, Z.; Lin, M.; Lin, H.; Huang, M. Facile Synthesis of Cellulose Nanofiber Nanocomposite as a SERS Substrate for Detection of Thiram in Juice. *Carbohydr. Polym.* **2018**, *189*, 79–86. DOI: 10.1016/j.carbpol.2018.02.014.
[66] Chamuah, N.; Bhuyan, N.; Das, P. P.; Ojah, N.; Choudhary, A. J.; Medhi, T.; Nath, P. Gold-Coated Electrospun PVA Nanofibers as SERS Substrate for Detection of Pesticides. *Sens. Actuators B Chem* **2018**, *273*, 710–717. DOI: 10.1016/j.snb.2018.06.079.
[67] Hao, J.; Han, M.-J.; Han, S.; Meng, X.; Su, T.-L.; Wang, Q. K. SERS Detection of Arsenic in Water: A Review. *J Environ Sci (China)* **2015**, *36*, 152–162. DOI: 10.1016/j.jes.2015.05.013.
[68] Shi, Y.; Wang, H.; Jiang, X.; Sun, B.; Song, B.; Su, Y.; He, Y. Ultrasensitive, Specific, Recyclable, and Reproducible Detection of Lead Ions in Real Systems through a Polyadenine-Assisted, Surface-Enhanced Raman Scattering Silicon Chip. *Anal. Chem.* **2016**, *88*, 3723–3729. DOI: 10.1021/acs.analchem.5b04551.
[69] David, C.; Guillot, N.; Shen, H.; Toury, T.; de la Chapelle, M. L. SERS Detection of Biomolecules Using Lithographed Nanoparticles towards a Reproducible SERS Biosensor. *Nanotechnology* **2010**, *21*, 475501. DOI: 10.1088/0957-4484/21/47/475501.
[70] Neng, J.; Harpster, M. H.; Wilson, W. C.; Johnson, P. A. Surface-Enhanced Raman Scattering (SERS) Detection of Multiple Viral Antigens Using Magnetic Capture of SERS-Active Nanoparticles. *Biosens. Bioelectron.* **2013**, *41*, 316–321. DOI: 10.1016/j.bios.2012.08.048.
[71] Guselnikova, O.; Lim, H.; Na, J.; Eguchi, M.; Kim, H.-J.; Elashnikov, R.; Postnikov, P.; Svorcik, V.; Semyonov, O.; Miliutina, E.; et al. Enantioselective SERS Sensing of Pseudoephedrine in Blood Plasma Biomatrix by Hierarchical Mesoporous Au Films Coated with a Homochiral MOF. *Biosens. Bioelectron.* **2021**, *180*, 113109. DOI: 10.1016/j.bios.2021.113109.
[72] Alvarez-Puebla, R. A.; Liz-Marzán, L. M. SERS Detection of Small Inorganic Molecules and Ions. *Angew. Chem. Int. Ed. Engl.* **2012**, *51*, 11214–11223. DOI: 10.1002/anie.201204438.
[73] Pang, S.; Yang, T.; He, L. Review of Surface Enhanced Raman Spectroscopic (SERS) Detection of Synthetic Chemical Pesticides. *Trends Analyt. Chem* **2016**, *85*, 73–82. DOI: 10.1016/j.trac.2016.06.017.
[74] Fazio, B.; D'Andrea, C.; Foti, A.; Messina, E.; Irrera, A.; Donato, M. G.; Villari, V.; Micali, N.; Maragò, O. M.; Gucciardi, P. G. SERS Detection of Biomolecules at Physiological pH via Aggregation of Gold Nanorods Mediated by Optical Forces and Plasmonic Heating. *Sci. Rep.* **2016**, *6*, 26952. DOI: 10.1038/srep26952.
[75] Spadaro, D.; Iatí, M. A.; Pérez-Piñeiro, J.; Vázquez-Vázquez, C.; Correa-Duarte, M. A.; Donato, M. G.; Gucciardi, P. G.; Saija, R.; Strangi, G.; Maragò, O. M. Optical Trapping of Plasmonic Mesocapsules: Enhanced Optical Forces and SERS. *J. Phys. Chem. C* **2017**, *121*, 691–700. DOI: 10.1021/acs.jpcc.6b10213.
[76] Lin, L.; Peng, X.; Wang, M.; Scarabelli, L.; Mao, Z.; Liz-Marzán, L. M.; Becker, M. F.; Zheng, Y. Light-Directed Reversible Assembly of Plasmonic Nanoparticles Using Plasmon-Enhanced Thermophoresis. *ACS Nano.* **2016**, *10*, 9659–9668. DOI: 10.1021/acsnano.6b05486.
[77] Fusco, Z.; Bo, R.; Wang, Y.; Motta, N.; Chen, H.; Tricoli, A. Self-Assembly of Au Nano-Islands with Tuneable Organized Disorder for Highly Sensitive SERS. *J. Mater. Chem. C* **2019**, *7*, 6308–6316. DOI: 10.1039/C9TC01231A.
[78] Li, J.; Zheng, Y. Optothermally Assembled Nanostructures. *Acc. Mater. Res.* **2021**, *2*, 352–363. DOI: 10.1021/accountsmr.1c00033.
[79] Xu, M.-L.; Gao, Y.; Han, X. X.; Zhao, B. Detection of Pesticide Residues in Food Using Surface-Enhanced Raman Spectroscopy: A Review. *J. Agric. Food Chem.* **2017**, *65*, 6719–6726. DOI: 10.1021/acs.jafc.7b02504.
[80] Lai, Y.-C.; Ho, H.-C.; Shih, B.-W.; Tsai, F.-Y.; Hsueh, C.-H. High Performance and Reusable SERS Substrates Using Ag/ZnO Heterostructure on Periodic Silicon Nanotube Substrate. *Appl. Surf. Sci* **2018**, *439*, 852–858. DOI: 10.1016/j.apsusc.2018.01.092.
[81] Gill, H. S.; Thota, S.; Li, L.; Ren, H.; Mosurkal, R.; Kumar, J. Reusable SERS Active Substrates for Ultrasensitive Molecular Detection. *Sens. Actuators B Chem* **2015**, *220*, 794–798. DOI: 10.1016/j.snb.2015.05.114.
[82] Ma, L.; Huang, Y.; Hou, M.; Xie, Z.; Zhang, Z. Ag Nanorods Coated with Ultrathin TiO2 Shells as Stable and Recyclable SERS Substrates. *Sci. Rep.* **2015**, *5*, 15442. DOI: 10.1038/srep15442.
[83] Braun, G. B.; Lee, S. J.; Laurence, T.; Fera, N.; Fabris, L.; Bazan, G. C.; Moskovits, M.; Reich, N. O. Generalized Approach to SERS-Active Nanomaterials via Controlled

Nanoparticle Linking, Polymer Encapsulation, and Small-Molecule Infusion. *J. Phys. Chem. C* **2009**, *113*, 13622–13629. DOI: 10.1021/jp903399p.

[84] Kalachyova, Y.; Mares, D.; Jerabek, V.; Ulbrich, P.; Lapcak, L.; Svorcik, V.; Lyutakov, O. Ultrasensitive and Reproducible SERS Platform of Coupled Ag Grating with Multibranched Au Nanoparticles. *Phys. Chem. Chem. Phys.* **2017**, *19*, 14761–14769. DOI: 10.1039/c7cp01828b.

[85] Wang, Y.; Tang, L.-J.; Jiang, J.-H. Surface-Enhanced Raman Spectroscopy-Based, Homogeneous, Multiplexed Immunoassay with Antibody-Fragments-Decorated Gold Nanoparticles. *Anal. Chem.* **2013**, *85*, 9213–9220. DOI: 10.1021/ac4019439.

[86] Cao, X.; Hong, S.; Jiang, Z.; She, Y.; Wang, S.; Zhang, C.; Li, H.; Jin, F.; Jin, M.; Wang, J. SERS-Active Metal-Organic Frameworks with Embedded Gold Nanoparticles. *Analyst* **2017**, *142*, 2640–2647. DOI: 10.1039/c7an00534b.

[87] Alvarez-Puebla, R. A.; Liz-Marzán, L. M. Traps and Cages for Universal SERS Detection. *Chem. Soc. Rev.* **2012**, *41*, 43–51. DOI: 10.1039/c1cs15155j.

[88] Lin, X.-M.; Cui, Y.; Xu, Y.-H.; Ren, B.; Tian, Z.-Q. Surface-Enhanced Raman Spectroscopy: Substrate-Related Issues. *Anal. Bioanal. Chem.* **2009**, *394*, 1729–1745. DOI: 10.1007/s00216-009-2761-5.

[89] Tao, A.; Sinsermsuksakul, P.; Yang, P. Tunable Plasmonic Lattices of Silver Nanocrystals. *Nat. Nanotechnol.* **2007**, *2*, 435–440. DOI: 10.1038/nnano.2007.189.

[90] Wu, D.-Y.; Li, J.-F.; Ren, B.; Tian, Z.-Q. Electrochemical Surface-Enhanced Raman Spectroscopy of Nanostructures. *Chem. Soc. Rev.* **2008**, *37*, 1025–1041. DOI: 10.1039/b707872m.

[91] Grys, D.-B.; Chikkaraddy, R.; Kamp, M.; Scherman, O. A.; Baumberg, J. J.; Nijs, B. Eliminating Irreproducibility in SERS Substrates. *J. Raman Spectrosc.* **2021**, *52*, 412–419. DOI: 10.1002/jrs.6008.

[92] Fales, A. M.; Vo-Dinh, T. Silver Embedded Nanostars for SERS with Internal Reference (SENSIR). *J. Mater. Chem. C* **2015**, *3*, 7319–7324. DOI: 10.1039/C5TC01296A.

[93] Prakash, V.; Rodriguez, R. D.; Al-Hamry, A.; Lipovka, A.; Dorozhko, E.; Selyshchev, O.; Ma, B.; Sharma, S.; Mehta, S. K.; Dzhagan, V.; et al. Flexible Plasmonic Graphene Oxide/Heterostructures for Dual-Channel Detection. *Analyst* **2019**, *144*, 3297–3306. DOI: 10.1039/c8an02495b.

[94] Castaño-Guerrero, Y.; Moreira, F. T. C.; Sousa-Castillo, A.; Correa-Duarte, M. A.; Sales, M. G. F. SERS and Electrochemical Impedance Spectroscopy Immunoassay for Carcinoembryonic Antigen. *Electrochim. Acta* **2021**, *366*, 137377. DOI: 10.1016/j.electacta.2020.137377.

[95] Ibáñez, D.; Pérez-Junquera, A.; González-García, M. B.; Hernández-Santos, D.; Fanjul-Bolado, P. Spectroelectrochemical Elucidation of B Vitamins Present in Multivitamin Complexes by EC-SERS. *Talanta* **2020**, *206*, 120190. DOI: 10.1016/j.talanta.2019.120190.

[96] Sanger, K.; Durucan, O.; Wu, K.; Thilsted, A. H.; Heiskanen, A.; Rindzevicius, T.; Schmidt, M. S.; Zór, K.; Boisen, A. Large-Scale, Lithography-Free Production of Transparent Nanostructured Surface for Dual-Functional Electrochemical and SERS Sensing. *ACS Sens.* **2017**, *2*, 1869–1875. DOI: 10.1021/acssensors.7b00783.

[97] Wei, W.; Lin, H.; Hao, T.; Su, X.; Jiang, X.; Wang, S.; Hu, Y.; Guo, Z. Dual-Mode ECL/SERS Immunoassay for Ultrasensitive Determination of Vibrio Vulnificus Based on Multifunctional MXene. *Sens. Actuators, B* **2021**, *332*, 129525. DOI: 10.1016/j.snb.2021.129525.

[98] Ameku, W. A.; de Araujo, W. R.; Rangel, C. J.; Ando, R. A.; Paixão, T. R. L. C. Gold Nanoparticle Paper-Based Dual-Detection Device for Forensics Applications. *ACS Appl. Nano Mater.* **2019**, *2*, 5460–5468. DOI: 10.1021/acsanm.9b01057.

[99] Devasenathipathy, R.; Rani, K. K.; Liu, J.; Wu, D.-Y.; Tian, Z.-Q. Plasmon Mediated Photoelectrochemical Transformations: The Example of Para-Aminothiophenol. *Electrochim. Acta* **2021**, *367*, 137485. DOI: 10.1016/j.electacta.2020.137485.

[100] Le Ru, E.; Etchegoin, P. *Principles of Surface-Enhanced Raman Spectroscopy: And Related Plasmonic Effects*; Elsevier: New York, NY, **2008**. [Database][Mismatch

[101] Zheng, X.; Zhang, L.; Huang, L.; Li, W.; Ma, C.; Song, R.; Chen, L.; Zeng, H. Optical Sensor Assistant with Voltage Enrichment for Ultrasensitive Detection of Mercury Ions. *ACS Omega.* **2019**, *4*, 6175–6179. DOI: 10.1021/acsomega.8b03505.

[102] Wang, L.; Gan, Z.-F.; Guo, D.; Xia, H.-L.; Patrice, F. T.; Hafez, M. E.; Li, D.-W. Electrochemistry-Regulated Recyclable SERS Sensor for Sensitive and Selective Detection of Tyrosinase Activity. *Anal. Chem.* **2019**, *91*, 6507–6513. DOI: 10.1021/acs.analchem.8b05341.

[103] Lacharmoise, P. D.; Le Ru, E. C.; Etchegoin, P. G. Guiding Molecules with Electrostatic Forces in Surface Enhanced Raman Spectroscopy. *ACS Nano.* **2009**, *3*, 66–72. DOI: 10.1021/nn800710m.

[104] Bindesri, S. D.; Alhatab, D. S.; Brosseau, C. L. Development of an Electrochemical Surface-Enhanced Raman Spectroscopy (EC-SERS) Fabric-Based Plasmonic Sensor for Point-of-Care Diagnostics. *Analyst* **2018**, *143*, 4128–4135. DOI: 10.1039/c8an01117f.

[105] Zaleski, S.; Cardinal, M. F.; Chulhai, D. V.; Wilson, A. J.; Willets, K. A.; Jensen, L.; Van Duyne, R. P. Toward Monitoring Electrochemical Reactions with Dual-Wavelength SERS: Characterization of Rhodamine 6G (R6G) Neutral Radical Species and Covalent Tethering of R6G to Silver Nanoparticles. *J. Phys. Chem. C* **2016**, *120*, 24982–24991. DOI: 10.1021/acs.jpcc.6b09022.

[106] Li, D.; Li, D.-W.; Fossey, J. S.; Long, Y.-T. Portable Surface-Enhanced Raman Scattering Sensor for Rapid Detection of Aniline and Phenol Derivatives by on-Site Electrostatic Preconcentration. *Anal. Chem.* **2010**, *82*, 9299–9305. DOI: 10.1021/ac101812x.

[107] Lian, W.; Wang, L.; Song, Y.; Yuan, H.; Zhao, S.; Li, P.; Chen, L. A Hydrogen Peroxide Sensor Based on Electrochemically Roughened Silver Electrodes. *Electrochim. Acta* **2009**, *54*, 4334–4339. DOI: 10.1016/j.electacta.2009.02.106.

[108] Yang, H.; Liu, C.; Tang, J.; Jin, W.; Hao, X.; Ji, X.; Hu, J. Twinned Copper Nanoparticles Modulated with Electrochemical Deposition for in Situ SERS Monitoring. *CrystEngComm* **2018**, *20*, 5609–5618. DOI: 10.1039/C8CE01009A.

[109] An, H.; Wu, L.; Mandemaker, L. D. B.; Yang, S.; Ruiter, J.; Wijten, J. H. J.; Janssens, J. C. L.; Hartman, T.; Stam, W.; Weckhuysen, B. M. Sub-Second Time-Resolved Surface-Enhanced Raman Spectroscopy Reveals Dynamic CO Intermediates during Electrochemical CO Reduction on Copper. *Angew. Chem. Int. Ed.* **2021**, *60*, 16576–16584. DOI: 10.1002/anie.202104114.

[110] Gieseking, R. L. M.; Lee, J.; Tallarida, N.; Apkarian, V. A.; Schatz, G. C. Bias-Dependent Chemical Enhancement and Nonclassical Stark Effect in Tip-Enhanced Raman Spectromicroscopy of CO-Terminated Ag Tips. *J. Phys. Chem. Lett.* **2018**, *9*, 3074–3080. DOI: 10.1021/acs.jpclett.8b01343.

[111] Hill, W.; Wehling, B. Potential- and pH-Dependent Surface-Enhanced Raman Scattering of P-Mercapto Aniline on Silver and Gold Substrates. *J. Phys. Chem.* **1993**, *97*, 9451–9455. DOI: 10.1021/j100139a032.

[112] Optical-Electrical Synergy on Electricity Manipulating Plasmon-Driven Photoelectrical Catalysis. *Appl. Mater. Today* **2019**, *15*, 305–314.

[113] Zhao, J.; Zhang, C.; Lu, Y.; Wu, Q.; Yuan, Y.; Xu, M.; Yao, J. Surface-Enhanced Raman Spectroscopic Investigation on Surface Plasmon Resonance and Electrochemical Catalysis on Surface Coupling Reaction of Pyridine at Au/TiO 2 Junction Electrodes. *J. Raman Spectrosc.* **2020**, *51*, 2199–2207. DOI: 10.1002/jrs.5982.

[114] Ding, S.-Y.; Yi, J.; Li, J.-F.; Tian, Z.-Q. A Theoretical and Experimental Approach to Shell-Isolated Nanoparticle-Enhanced Raman Spectroscopy of Single-Crystal Electrodes. *Surf. Sci.* **2015**, *631*, 73–80. DOI: 10.1016/j.susc.2014.07.019.

[115] Xie, L.-Q.; Ding, D.; Zhang, M.; Chen, S.; Qiu, Z.; Yan, J.-W.; Yang, Z.-L.; Chen, M.-S.; Mao, B.-W.; Tian, Z.-Q. Adsorption of Dye Molecules on Single Crystalline Semiconductor Surfaces: An Electrochemical Shell-Isolated Nanoparticle Enhanced Raman Spectroscopy Study. *J. Phys. Chem. C* **2016**, *120*, 22500–22507. DOI: 10.1021/acs.jpcc.6b07763.

[116] Dong, J.-C.; Panneerselvam, R.; Lin, Y.; Tian, X.-D.; Li, J.-F. Shell-Isolated Nanoparticle-Enhanced Raman Spectroscopy at Single-Crystal Electrode Surfaces. *Adv. Opt. Mater.* **2016**, *4*, 1144–1158. DOI: 10.1002/adom.201600223.

[117] Li, C.-Y.; Yang, Z.-W.; Dong, J.-C.; Ganguly, T.; Li, J.-F. Plasmon-Enhanced Spectroscopy: Plasmon-Enhanced Spectroscopies with Shell-Isolated Nanoparticles (Small 8/2017). *Small* **2017**, *13*, 1601598. DOI: 10.1002/smll.201770043.

[118] León, L.; Mozo, J. D. Designing Spectroelectrochemical Cells: A Review. *TrAC - Trends Anal. Chem.* **2018**, *102*, 147–169. DOI: 10.1016/j.trac.2018.02.002.

[119] Karoń, K.; Łapkowski, M.; Dobrowolski, J. C. ECD Spectroelectrochemistry: A Review. *Spectrochim. Acta. A Mol. Biomol. Spectrosc.* **2021**, *250*, 119349. DOI: 10.1016/j.saa.2020.119349.

[120] Robinson, A. M.; Harroun, S. G.; Bergman, J.; Brosseau, C. L. Portable Electrochemical Surface-Enhanced Raman Spectroscopy System for Routine Spectroelectrochemical Analysis. *Anal. Chem.* **2012**, *84*, 1760–1764. DOI: 10.1021/ac2030078.

[121] Rodriguez, R. D.; Shchadenko, S.; Murastov, G.; Lipovka, A.; Fatkullin, M.; Petrov, I.; Tran, T. -H.; Khalelov, A.; Saqib, M.; Villa, N. E.; et al. Ultra-Robust Flexible Electronics by Laser-Driven Polymer-Nanomaterials Integration. *Adv. Funct. Mater.* **2021**, *31*, 2008818. DOI: 10.1002/adfm.202008818.

[122] Touzalin, T.; Joiret, S.; Maisonhaute, E.; Lucas, I. T. Complex Electron Transfer Pathway at a Microelectrode Captured by in Situ Nanospectroscopy. *Anal. Chem.* **2017**, *89*, 8974–8980. DOI: 10.1021/acs.analchem.7b01542.

[123] Selimovic, A.; Johnson, A. S.; Kiss, I. Z.; Martin, R. S. Use of Epoxy-Embedded Electrodes to Integrate Electrochemical Detection with Microchip-Based Analysis Systems. *Electrophoresis* **2011**, *32*, 822–831. DOI: 10.1002/elps.201000665.

[124] Kang, G.; Yang, M.; Mattei, M. S.; Schatz, G. C.; Van Duyne, R. P. In Situ Nanoscale Redox Mapping Using Tip-Enhanced Raman Spectroscopy. *Nano Lett.* **2019**, *19*, 2106–2113. DOI: 10.1021/acs.nanolett.9b00313.

[125] Tsai, M.-H.; Lin, Y.-K.; Luo, S.-C. Electrochemical SERS for in Situ Monitoring the Redox States of PEDOT and Its Potential Application in Oxidant Detection. *ACS Appl. Mater. Interfaces.* **2019**, *11*, 1402–1410. DOI: 10.1021/acsami.8b16989.

[126] Niciński, K.; Witkowska, E.; Korsak, D.; Noworyta, K.; Trzcińska-Danielewicz, J.; Girstun, A.; Kamińska, A. Photovoltaic Cells as a Highly Efficient System for Biomedical and Electrochemical Surface-Enhanced Raman Spectroscopy Analysis. *RSC Adv.* **2019**, *9*, 576–591. DOI: 10.1039/C8RA08319C.

[127] Wang, Z.; Wang, W.; Liu, S.; Yang, N.; Zhao, G. Coupling Rotating Disk Electrodes and Surface-Enhanced Raman Spectroscopy for in Situ Electrochemistry Studies. *Electrochem. commun* **2021**, *124*, (106928. DOI: 10.1016/j.elecom.2021.106928.

[128] Becirovic, V.; Doonan, S. R.; Martin, R. S. Encapsulation of Fluidic Tubing and Microelectrodes in Microfluidic Devices: Integrating off-Chip Process and Coupling Conventional Capillary Electrophoresis with Electrochemical Detection. *Anal. Methods* **2013**, *5*, 4220–4229. DOI: 10.1039/C3AY40809D.

[129] Bailey, M. R.; Martin, R. S.; Schultz, Z. D. Role of Surface Adsorption in the Surface-Enhanced Raman Scattering and Electrochemical Detection of Neurotransmitters. *J. Phys. Chem. C Nanomater. Interfaces.* **2016**, *120*, 20624–20633. DOI: 10.1021/acs.jpcc.6b01196.

[130] Amemiya, S.; Bard, A. J.; Fan, F.-R. F.; Mirkin, M. V.; Unwin, P. R. Scanning Electrochemical Microscopy. *Annu Rev Anal Chem (Palo Alto Calif)* **2008**, *1*, 95–131. DOI: 10.1146/annurev.anchem.1.031207.112938.

[131] Sun, P.; Laforge, F. O.; Mirkin, M. V. Scanning Electrochemical Microscopy in the 21st Century. *Phys. Chem. Chem. Phys.* **2007**, *9*, 802–823. DOI: 10.1039/b612259k.

[132] Bao, Y.-F.; Cao, M.-F.; Wu, S.-S.; Huang, T.-X.; Zeng, Z.-C.; Li, M.-H.; Wang, X.; Ren, B. Atomic Force Microscopy Based Top-Illumination Electrochemical Tip-Enhanced Raman Spectroscopy. *Anal. Chem.* **2020**, *92*, 12548–12555. DOI: 10.1021/acs.analchem.0c02466.

[133] Touzalin, T.; Joiret, S.; Lucas, I. T.; Maisonhaute, E. Electrochemical Tip-Enhanced Raman Spectroscopy Imaging with 8 Nm Lateral Resolution. *Electrochem. Commun* **2019**, *108*, 106557. DOI: 10.1016/j.elecom.2019.106557.

[134] Huang, S.-C.; Wang, X.; Zhao, Q.-Q.; Zhu, J.-F.; Li, C.-W.; He, Y.-H.; Hu, S.; Sartin, M. M.; Yan, S.; Ren, B. Probing Nanoscale Spatial Distribution of Plasmonically Excited Hot Carriers. *Nat. Commun.* **2020**, *11*, 4211.

[135] Martín Sabanés, N.; Ohto, T.; Andrienko, D.; Nagata, Y.; Domke, K. F. Electrochemical TERS Elucidates Potential-Induced Molecular Reorientation of Adenine/Au(111). *Angew. Chem.* **2017**, *129*, 9928–9933. DOI: 10.1002/ange.201704460.

[136] Zeng, Z.-C.; Huang, S.-C.; Wu, D.-Y.; Meng, L.-Y.; Li, M.-H.; Huang, T.-X.; Zhong, J.-H.; Wang, X.; Yang, Z.-L.; Ren, B. Electrochemical Tip-Enhanced Raman Spectroscopy. *J. Am. Chem. Soc.* **2015**, *137*, 11928–11931. DOI: 10.1021/jacs.5b08143.

[137] Gu, X.; Wang, K.; Qiu, J.; Wang, Y.; Tian, S.; He, Z.; Zong, R.; Kraatz, H.-B. Enhanced Electrochemical and SERS Signals by Self-Assembled Gold Microelectrode Arrays: A Dual Readout Platform for Multiplex Immumoassay of Tumor Biomarkers. *Sens. Actuators B Chem* **2021**, *334*, 129674. DOI: 10.1016/j.snb.2021.129674.

[138] Zhou, H.; Zhang, J.; Li, B.; Liu, J.; Xu, J.-J.; Chen, H.-Y. Dual-Mode SERS and Electrochemical Detection of miRNA Based on Popcorn-like Gold Nanofilms and Toehold-Mediated Strand Displacement Amplification Reaction. *Anal. Chem.* **2021**, *93*, 6120–6127. DOI: 10.1021/acs.analchem.0c05221.

[139] Ilkhani, H.; Hughes, T.; Li, J.; Zhong, C. J.; Hepel, M. Nanostructured SERS-Electrochemical Biosensors for Testing of Anticancer Drug Interactions with DNA. *Biosens. Bioelectron.* **2016**, *80*, 257–264. DOI: 10.1016/j.bios.2016.01.068.

[140] Do, H.; Kwon, S.-R.; Fu, K.; Morales-Soto, N.; Shrout, J. D.; Bohn, P. W. Electrochemical Surface-Enhanced Raman Spectroscopy of Pyocyanin Secreted by Pseudomonas Aeruginosa Communities. *Langmuir* **2019**, *35*, 7043–7049. DOI: 10.1021/acs.langmuir.9b00184.

[141] McLeod, K. E. R.; Lynk, T. P.; Sit, C. S.; Brosseau, C. L. On the Origin of Electrochemical Surface-Enhanced Raman Spectroscopy (EC-SERS) Signals for Bacterial Samples: The Importance of Filtered Control Studies in the Development of New Bacterial Screening Platforms. *Anal. Methods* **2019**, *11*, 924–929. DOI: 10.1039/C8AY02613K.

[142] Zhao, L.; Blackburn, J.; Brosseau, C. L. Quantitative Detection of Uric Acid by Electrochemical-Surface Enhanced Raman Spectroscopy Using a Multilayered Au/Ag Substrate. *Anal. Chem.* **2015**, *87*, 441–447. DOI: 10.1021/ac503967s.

[143] Hassanain, W. A.; Izake, E. L.; Ayoko, G. A. Spectroelectrochemical Nanosensor for the Determination of Cystatin C in Human Blood. *Anal. Chem.* **2018**, *90*, 10843–10850. DOI: 10.1021/acs.analchem.8b02121.

[144] Karaballi, R. A.; Nel, A.; Krishnan, S.; Blackburn, J.; Brosseau, C. L. Development of an Electrochemical Surface-Enhanced Raman Spectroscopy (EC-SERS) Aptasensor for Direct Detection of DNA Hybridization. *Phys. Chem. Chem. Phys.* **2015**, *17*, 21356–21363. DOI: 10.1039/c4cp05077k.

[145] Zhao, J.; Liang, D.; Gao, S.; Hu, X.; Koh, K.; Chen, H. Analyte-Resolved Magnetoplasmonic Nanocomposite to Enhance SPR Signals and Dual Recognition Strategy for Detection of BNP in Serum Samples. *Biosens. Bioelectron.* **2019**, *141*, 111440. DOI: 10.1016/j.bios.2019.111440.

[146] Greene, B. H. C.; Alhatab, D. S.; Pye, C. C.; Brosseau, C. L. Electrochemical-Surface Enhanced Raman Spectroscopic (EC-SERS) Study of 6-Thiouric Acid: A Metabolite of the Chemotherapy Drug Azathioprine. *J. Phys. Chem. C* **2017**, *121*, 8084–8090. DOI: 10.1021/acs.jpcc.7b01179.

[147] Velička, M.; Zacharovas, E.; Adomavičiūtė, S.; Šablinskas, V. Detection of caffeine intake by Means of EC-SERS Spectroscopy of Human Saliva. *Spectrochim. Acta. A Mol. Biomol. Spectrosc.* **2021**, *246*, 118956. DOI: 10.1016/j.saa.2020.118956.

[148] Balaji, R.; Maheshwaran, S.; Chen, S.-M.; Chandrasekar, N.; Ethiraj, S.; Samuel, M. S.; Renganathan, V. High-Performance Catalytic Strips Assembled with BiOBr Nano-Rose Architectures for Electrochemical and SERS Detection of Theophylline. *Chemical Engineering Journal* **2021**, *425*, 130616. DOI: 10.1016/j.cej.2021.130616.

[149] Zaleski, S.; Clark, K. A.; Smith, M. M.; Eilert, J. Y.; Doty, M.; Van Duyne, R. P. Identification and Quantification of Intravenous Therapy Drugs Using Normal Raman Spectroscopy and Electrochemical Surface-Enhanced Raman Spectroscopy. *Anal. Chem.* **2017**, *89*, 2497–2504. DOI: 10.1021/acs.analchem.6b04636.

[150] Kayran, Y. U.; Jambrec, D.; Schuhmann, W. Nanostructured DNA Microarrays for Dual SERS and Electrochemical Read-Out. *Electroanalysis* **2019**, *31*, 267–272. DOI: 10.1002/elan.201800579.

[151] Zhou, J.; Yang, D.; Liu, G.; Li, S.; Feng, W.; Yang, G.; He, J.; Shan, Y. Highly Sensitive Detection of DNA Damage in Living Cells by SERS and Electrochemical Measurements Using a Flexible Gold Nanoelectrode. *Analyst* **2021**, *146*, 2321–2329. DOI: 10.1039/d1an00220a.

[152] Pomerantseva, E.; Bonaccorso, F.; Feng, X.; Cui, Y.; Gogotsi, Y. Energy Storage: The Future Enabled by Nanomaterials. *Science* **2019**, *366*, eaan8285. DOI: 10.1126/science.aan8285.

[153] Singh, J.; Juneja, S.; Ghosal, A.; Ghosal, A. Energy Harvesting: Role of Plasmonic Nanocomposites for Energy Efficient Devices. In *Integrating Green Chemistry and Sustainable Engineering*; Wiley: Hoboken, NJ, **2019**; pp 81–112.

[154] Zhang, P.; Zeng, G.; Song, T.; Huang, S.; Wang, T.; Zeng, H. Design of Plasmonic CuCo Bimetal as a Nonsemiconductor Photocatalyst for Synchronized Hydrogen Evolution and Storage. *Appl. Catal. B* **2019**, *242*, 389–396. DOI: 10.1016/j.apcatb.2018.10.020.

[155] Yasmeen, H.; Zada, A.; Ali, S.; Khan, I.; Ali, W.; Khan, W.; Khan, M.; Anwar, N.; Ali, A.; Huerta-Flores, A. M.; Subhan, F. Visible Light-Excited Surface Plasmon Resonance Charge Transfer Significantly Improves the Photocatalytic Activities of ZnO Semiconductor for Pollutants Degradation. *J. Chin. Chem. Soc.* **2020**, *67*, 1611–1617. DOI: 10.1002/jccs.202000205.

[156] Yue, X.; Hou, J.; Zhang, Y.; Wu, P.; Guo, Y.; Peng, S.; Liu, Z.; Jiang, H. Improved CdS Photocatalytic H Evolution Using Au-Ag Nanoparticles with Tunable Plasmon-Enhanced Resonance Energy Transfer. *Dalton Trans.* **2020**, *49*, 7467–7473. DOI: 10.1039/d0dt01110j.

[157] Zhang, P.; Liu, H.; Li, X. Photo-Reduction Synthesis of Cu Nanoparticles as Plasmon-Driven Non-Semiconductor Photocatalyst for Overall Water Splitting. *Appl. Surf. Sci* **2021**, *535*, (147720. DOI: 10.1016/j.apsusc.2020.147720.

[158] Vahidzadeh, E.; Zeng, S.; Manuel, A. P.; Riddell, S.; Kumar, P.; Alam, K. M.; Shankar, K. Asymmetric Multipole Plasmon-Mediated Catalysis Shifts the Product Selectivity of CO Photoreduction toward C Products. *ACS Appl. Mater. Interfaces.* **2021**, *13*, 7248–7258. DOI: 10.1021/acsami.0c21067.

[159] Li, S.; Miao, P.; Zhang, Y.; Wu, J.; Zhang, B.; Du, Y.; Han, X.; Sun, J.; Xu, P. Recent Advances in Plasmonic Nanostructures for Enhanced Photocatalysis and Electrocatalysis. *Adv. Mater.* **2021**, *33*, e2000086. DOI: 10.1002/adma.202000086.

[160] Marchuk, K.; Willets, K. A. Localized Surface Plasmons and Hot Electrons. *Chem. Phys* **2014**, *445*, 95–104. DOI: 10.1016/j.chemphys.2014.10.016.

[161] Boerigter, C.; Aslam, U.; Linic, S. Mechanism of Charge Transfer from Plasmonic Nanostructures to Chemically Attached Materials. *ACS Nano.* **2016**, *10*, 6108–6115. DOI: 10.1021/acsnano.6b01846.

[162] Zhang, L.; Mohamed, H. H.; Dillert, R.; Bahnemann, D. Kinetics and Mechanisms of Charge Transfer Processes in Photocatalytic Systems: A Review. *J. Photochem. Photobiol. C: Photochem. Rev* **2012**, *13*, 263–276. DOI: 10.1016/j.jphotochemrev.2012.07.002.

[163] Golubev, A. A.; Khlebtsov, B. N.; Rodriguez, R. D.; Chen, Y.; Zahn, D. R. T. Plasmonic Heating Plays a Dominant Role in the Plasmon-Induced Photocatalytic Reduction of 4-Nitrobenzenethiol. *J. Phys. Chem. C* **2018**, *122*, 5657–5663. DOI: 10.1021/acs.jpcc.7b12101.

[164] Mascaretti, L.; Naldoni, A. Hot Electron and Thermal Effects in Plasmonic Photocatalysis. *J. Appl. Phys* **2020**, *128*, 041101. DOI: 10.1063/5.0013945.

[165] Dubi, Y.; Un, I. W.; Sivan, Y. Thermal Effects—An Alternative Mechanism for Plasmon-Assisted Photocatalysis. *Chem. Sci.* **2020**, *11*, 5017–5027. DOI: 10.1039/c9sc06480j.

[166] Wang, X.; Xu, Z.; Gao, X. An Electrochemical and Raman Spectroscopic Study on Involvement of La3+ Ions in Lactate Dehydrogenase Catalysis. *Chin. Sci. Bull.* **1998**, *43*, 1625–1630. DOI: 10.1007/BF02883407.

[167] Li, X.; Zhang, C.; Wu, Q.; Zhang, J.; Xu, M.; Yuan, Y.; Yao, J. In Situ Surface-Enhanced Raman Spectroscopic Monitoring Electrochemical and Surface Plasmon Resonance Synergetic Catalysis on Dehydroxylation of PHTP at Ag Electrodes. *J. Raman Spectrosc.* **2018**, *49*, 1928–1937. DOI: 10.1002/jrs.5478.

[168] Huang, Y.-F.; Zhu, H.-P.; Liu, G.-K.; Wu, D.-Y.; Ren, B.; Tian, Z.-Q. When the Signal is Not from the Original Molecule to Be Detected: Chemical Transformation of Para-Aminothiophenol on Ag during the SERS Measurement. *J. Am. Chem. Soc.* **2010**, *132*, 9244–9246. DOI: 10.1021/ja101107z.

[169] Cui, L.; Wang, P.; Fang, Y.; Li, Y.; Sun, M. A Plasmon-Driven Selective Surface Catalytic Reaction Revealed by Surface-Enhanced Raman Scattering in an Electrochemical Environment. *Sci. Rep* **2015**, *5*, 11920.

[170] Wang, Y.-H.; Wei, J.; Radjenovic, P.; Tian, Z.-Q.; Li, J.-F. In Situ Analysis of Surface Catalytic Reactions Using Shell-Isolated Nanoparticle-Enhanced Raman Spectroscopy. *Anal. Chem.* **2019**, *91*, 1675–1685. DOI: 10.1021/acs.analchem.8b05499.

[171] Chen, J.; Liu, G.; Zhu, Y.-Z.; Su, M.; Yin, P.; Wu, X.-J.; Lu, Q.; Tan, C.; Zhao, M.; Liu, Z.; et al. Ag@MoS Core-Shell Heterostructure as SERS Platform to Reveal the Hydrogen Evolution Active Sites of Single-Layer MoS. *J. Am. Chem. Soc.* **2020**, *142*, 7161–7167. DOI: 10.1021/jacs.0c01649.

[172] Gao, M.-R.; Chan, M. K. Y.; Sun, Y. Edge-Terminated Molybdenum Disulfide with a 9.4-Å Interlayer Spacing for Electrochemical Hydrogen Production. *Nat. Commun.* **2015**, *6*, 7493.

[173] Tang, Q.; Jiang, D.-E. Mechanism of Hydrogen Evolution Reaction on 1T-MoS2 from First Principles. *ACS Catal.* **2016**, *6*, 4953–4961. DOI: 10.1021/acscatal.6b01211.

[174] Deng, Y.; Ting, L. R. L.; Neo, P. H. L.; Zhang, Y.-J.; Peterson, A. A.; Yeo, B. S. Operando Raman Spectroscopy of Amorphous Molybdenum Sulfide (MoSx) during the Electrochemical Hydrogen Evolution Reaction: Identification of Sulfur Atoms as Catalytically Active Sites for H + Reduction. *ACS Catal.* **2016**, *6*, 7790–7798. DOI: 10.1021/acscatal.6b01848.

[175] Sengupta, K.; Chatterjee, S.; Dey, A. In Situ Mechanistic Investigation of O2 Reduction by Iron Porphyrin Electrocatalysts Using Surface-Enhanced Resonance Raman Spectroscopy Coupled to Rotating Disk Electrode (SERRS-RDE) Setup. *ACS Catal.* **2016**, *6*, 6838–6852. DOI: 10.1021/acscatal.6b01122.

[176] Yeo, B. S.; Klaus, S. L.; Ross, P. N.; Mathies, R. A.; Bell, A. T. Identification of Hydroperoxy Species as Reaction Intermediates in the Electrochemical Evolution of Oxygen on Gold. *Chemphyschem* **2010**, *11*, 1854–1857. DOI: 10.1002/cphc.201000294.

[177] Wang, J.; Ma, L.; Xu, J.; Xu, Y.; Sun, K.; Peng, Z. Oxygen Electrochemistry in Li-O 2 Batteries Probed by in Situ Surface-Enhanced Raman Spectroscopy. *SusMat* **2021**, *1*, 345–358. DOI: 10.1002/sus2.24.

[178] In Situ Surface Enhanced Raman Spectroscopic Studies of Solid Electrolyte Interphase Formation in Lithium Ion Battery Electrodes. *J. Power Sources* **2014**, *256*, 324–328.

[179] Wang, J.; Zhang, Y.; Guo, L.; Wang, E.; Peng, Z. Identifying Reactive Sites and Transport Limitations of Oxygen Reactions in Aprotic Lithium-O2 Batteries at the Stage of Sudden Death. *Angew. Chem.* **2016**, *128*, 5287–5291. DOI: 10.1002/ange.201600793.

[180] In Situ Surface-Enhanced Raman Spectroscopy in Li–O2 Battery Research. *Curr. Opin. Electrochem.* **2019**, *17*, 174–183. DOI: 10.1016/j.coelec.2019.07.004.

[181] Liu, Q.; Tang, Y.; Sun, H.; Yang, T.; Sun, Y.; Du, C.; Jia, P.; Ye, H.; Chen, J.; Peng, Q.; et al. In Situ Electrochemical Study of Na–O2/CO2 Batteries in an Environmental Transmission Electron Microscope. *ACS Nano* **2020**, *14*, 13232–13245. DOI: 10.1021/acsnano.0c04938.

[182] Piernas-Muñoz, M. J.; Tornheim, A.; Trask, S.; Zhang, Z.; Bloom, I. Surface-Enhanced Raman Spectroscopy (SERS): A Powerful Technique to Study the SEI Layer in Batteries. *Chem Commun (Camb)* **2021**, *57*, 2253–2256. DOI: 10.1039/d0cc08001b.

[183] Localized Surface Plasmon Resonance Enhanced Electrochemical Kinetics and Product Selectivity in Aprotic Li–O2 Batteries. *Energy Storage Mater.* **2021**, *42*, 618–627. DOI: 10.1016/j.ensm.2021.08.004.

[184] Wang, Y.-H.; Le, J.-B.; Li, W.-Q.; Wei, J.; Radjenovic, P. M.; Zhang, H.; Zhou, X.-S.; Cheng, J.; Tian, Z.-Q.; Li, J.-F. In Situ Spectroscopic Insight into the Origin of the Enhanced Performance of Bimetallic Nanocatalysts towards the Oxygen Reduction Reaction (ORR). *Angew. Chem.* **2019**, *131*, 16208–16212. DOI: 10.1002/ange.201908907.

[185] Dong, J.-C.; Zhang, X.-G.; Briega-Martos, V.; Jin, X.; Yang, J.; Chen, S.; Yang, Z.-L.; Wu, D.-Y.; Feliu, J. M.; Williams, C. T.; et al. In Situ Raman Spectroscopic Evidence for Oxygen Reduction Reaction Intermediates at Platinum Single-Crystal Surfaces. *Nat. Energy* **2019**, *4*, 60–67. DOI: 10.1038/s41560-018-0292-z.

[186] Wright, D.; Lin, Q.; Berta, D.; Földes, T.; Wagner, A.; Griffiths, J.; Readman, C.; Rosta, E.; Reisner, E.; Baumberg, J. J. Mechanistic Study of an Immobilized Molecular Electrocatalyst by in Situ Gap-Plasmon-Assisted Spectro-Electrochemistry. *Nat. Catal.* **2021**, *4*, 157–163. DOI: 10.1038/s41929-020-00566-x.

[187] Li, J.-F.; Zhang, Y.-J.; Rudnev, A. V.; Anema, J. R.; Li, S.-B.; Hong, W.-J.; Rajapandiyan, P.; Lipkowski, J.; Wandlowski, T.; Tian, Z.-Q. Electrochemical Shell-Isolated Nanoparticle-Enhanced Raman Spectroscopy: Correlating Structural Information and Adsorption Processes of Pyridine at the Au(Hkl) Single Crystal/Solution Interface. *J. Am. Chem. Soc.* **2015**, *137*, 2400–2408. DOI: 10.1021/ja513263j.

[188] Zhang, Y.-N.; Niu, Q.; Gu, X.; Yang, N.; Zhao, G. Recent Progress on Carbon Nanomaterials for the Electrochemical Detection and Removal of Environmental Pollutants. *Nanoscale* **2019**, *11*, 11992–12014. DOI: 10.1039/c9nr02935d.

[189] Surface Enhanced Raman Spectroscopy in Environmental Analysis, Monitoring and Assessment. *Sci. Total Environ* **2020**, *720*, 137601.

[190] A Novel Graphene-like Titanium Carbide MXene/Au–Ag Nanoshuttles Bifunctional Nanosensor for Electrochemical and SERS Intelligent Analysis of Ultra-Trace Carbendazim Coupled with Machine Learning. *Ceram. Int* **2021**, *47*, 173–184. DOI: 10.1016/j.ceramint.2020.08.121.

[191] Zhang, Y.; Seitz, W. R.; Grant, C. L.; Sundberg, D. C. A Clear, Amine-Containing Poly(Vinyl Chloride) Membrane for in Situ Optical Detection of 2,4,6-Trinitrotoluene. *Anal. Chim. Acta* **1989**, *217*, 217–227. DOI: 10.1016/S0003-2670(00)80404-3.

[192] Alizadeh, N.; Ghoorchian, A. Hybrid Optoelectrochemical Sensor for Superselective Detection of 2,4,6-Trinitrotoluene Based on Electrochemical Reduced Meisenheimer Complex. *Anal. Chem.* **2018**, *90*, 10360–10368. DOI: 10.1021/acs.analchem.8b02183.

[193] Liu, J.; Siavash Moakhar, R.; Mahshid, S.; Vasefi, F.; Wachsmann-Hogiu, S. Multimodal Electrochemical and SERS Platform for Chlorfenapyr Detection. *Appl. Surf. Sci* **2021**, *566*, 150617. DOI: 10.1016/j.apsusc.2021.150617.

[194] Sarfo, D. K.; Izake, E. L.; O'Mullane, A. P.; Ayoko, G. A. Molecular Recognition and Detection of Pb(II) Ions in Water by Aminobenzo-18-Crown-6 Immobilised onto a Nanostructured SERS Substrate. *Sens. Actuators B Chem* **2018**, *255*, 1945–1952. DOI: 10.1016/j.snb.2017.08.223.

[195] Esmaielzadeh Kandjani, A.; Sabri, Y. M.; Mohammad-Taheri, M.; Bansal, V.; Bhargava, S. K. Detect, Remove and Reuse: A New Paradigm in Sensing and Removal of Hg (II) from Wastewater via SERS-Active ZnO/Ag Nanoarrays. *Environ. Sci. Technol.* **2015**, *49*, 1578–1584. DOI: 10.1021/es503527e.

[196] Bonancêa, C. E.; do Nascimento, G. M.; de Souza, M. L.; Temperini, M. L. A.; Corio, P. Surface-Enhanced Raman Study of Electrochemical and Photocatalytic Degradation of the Azo Dye Janus Green B. *Appl. Catal. B* **2008**, *77*, 339–345. DOI: 10.1016/j.apcatb.2007.07.026.

[197] Eisnor, M. M.; McLeod, K. E. R.; Bindesri, S.; Svoboda, S. A.; Wustholz, K. L.; Brosseau, C. L. Electrochemical Surface-Enhanced Raman Spectroscopy (EC-SERS): A Tool for the Identification of Polyphenolic Components in Natural Lake Pigments. *Phys. Chem. Chem. Phys.* **2021**, *24*, 347–356. DOI: 10.1039/d1cp03301h.

[198] Silver Nanowires on Coffee Filter as Dual-Sensing Functionality for Efficient and Low-Cost SERS Substrate and Electrochemical Detection. *Sens. Actuators B Chem* **2017**, *245*, 189–195.

[199] Sarfo, D. K.; Izake, E. L.; O'Mullane, A. P.; Wang, T.; Wang, H.; Tesfamichael, T.; Ayoko, G. A. Fabrication of Dual Function Disposable Substrates for Spectroelectrochemical Nanosensing. *Sens. Actuators, B* **2019**, *287*, 9–17. DOI: 10.1016/j.snb.2019.02.012.

[200] Weng, C.; Luo, Y.; Wang, B.; Shi, J.; Gao, L.; Cao, Z.; Duan, G. Layer-Dependent SERS Enhancement of TiS2 Prepared by Simple Electrochemical Intercalation. *J. Mater. Chem. C* **2020**, *8*, 14138–14145. DOI: 10.1039/D0TC03683H.

[201] Petruš, O.; Oriňak, A.; Oriňaková, R.; Králová, Z. O.; Múdra, E.; Kupková, M.; Koval, K. Colloidal Lithography with Electrochemical Nickel Deposition as a Unique Method for Improved Silver Decorated Nanocavities in SERS Applications. *Appl. Surf. Sci.* **2017**, *423*, 322–330. DOI: 10.1016/j.apsusc.2017.06.149.

[202] Koh, C. S. L.; Lee, H. K.; Phan-Quang, G. C.; Han, X.; Lee, M. R.; Yang, Z.; Ling, X. Y. SERS- and Electrochemically Active 3D Plasmonic Liquid Marbles for Molecular-Level Spectroelectrochemical Investigation of Microliter Reactions. *Angew. Chem. Int. Ed. Engl.* **2017**, *56*, 8813–8817. DOI: 10.1002/anie.201704433.

[203] Wang, Y.-H.; Le, J.-B.; Li, W.-Q.; Wei, J.; Radjenovic, P. M.; Zhang, H.; Zhou, X.-S.; Cheng, J.; Tian, Z.-Q.; Li, J.-F. In Situ Spectroscopic Insight into the Origin of the Enhanced Performance of Bimetallic Nanocatalysts towards the Oxygen Reduction Reaction (ORR). *Angew. Chem. Int. Ed. Engl.* **2019**, *58*, 16062–16066. DOI: 10.1002/anie.201908907.